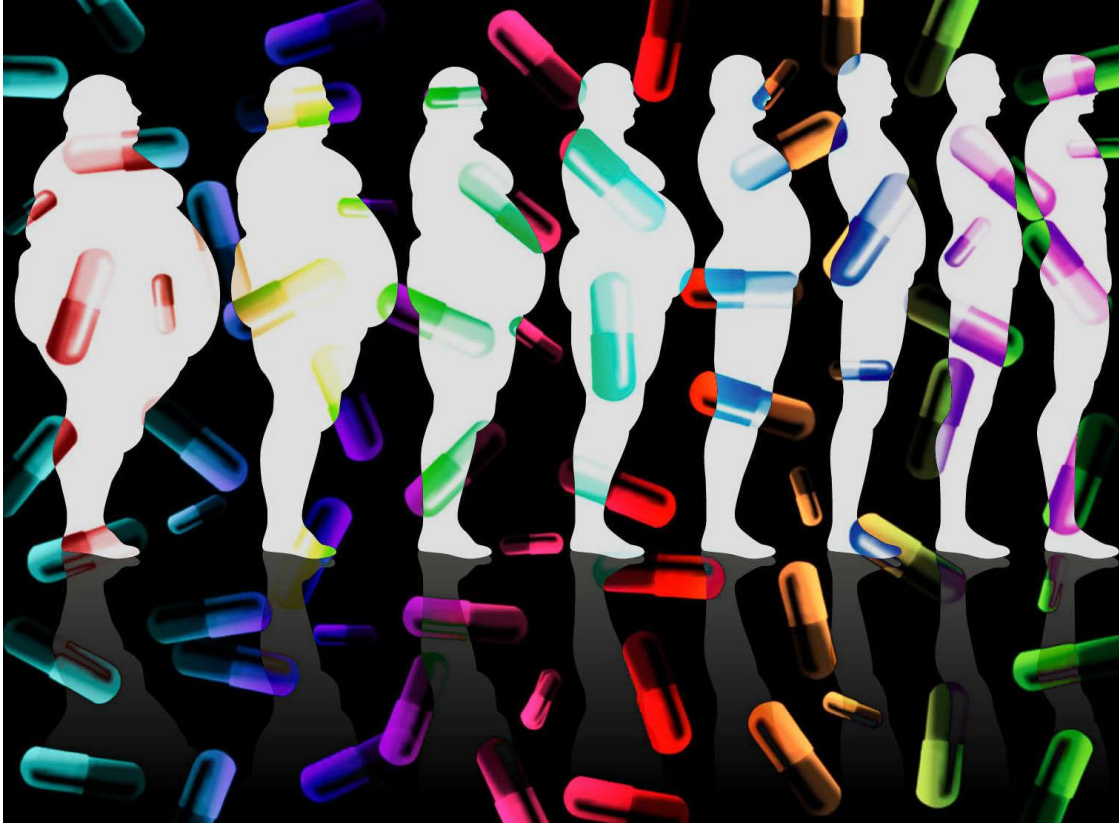# Cell type specificity in CB$_1$ antagonism

Remco Molenhuis
Research Project Thesis
Bachelor Biomedical Sciences
Utrecht University

R.T.Molenuis@students.uu.nl
Student number: 3384470

Supervisor: Dr. Geert Ramakers

Cell type specificity in CB_1 antagonism

Remco Molenhuis

Research Project Thesis
Bachelor Biomedical Sciences
Utrecht University

R.T.Molenuis@students.uu.nl
Student number: 3384470

Supervisor: Dr. Geert Ramakers

Abstract

Since the 1960s, much progress has been made in understanding *Cannabis sativa's* mechanism of action. Focus on CB_1, the G-protein coupled receptor held responsible for the psychoactive effects of marijuana and hashish, has led to multiple therapeutic applications. These include both appetite stimulation, by agonizing the receptor, and appetite reduction by antagonizing it. However, in the latter case, adverse have been noticed and the receptor seems to contain more complex properties than expected. These include constitute activity and possibly ligand specific activation of intracellular pathways. Utilizing these parameters in drug design might reduce adverse effects, while keeping the therapeutic force intact. Recently, astrocytes were shown to increase the release of neurotransmitters by endocannabinoids. This is in contrast with observations in neurons, where endocannabinoids show multiple forms of suppression of transmitter release. Activation of astrocytes by CB_1 was shown to be mediated by other G-proteins than usual in neurons. Therefore, cell type specific inhibition of endocannabinoids' effect is suggested to be possible. These results might be useful for further improving the balance between adverse and therapeutic effects of CB_1 antagonists.

Introduction

Cannabis sativa, its receptors and endogenous ligands

For many centuries marijuana and hashish were used both recreationally and medicinally, while their mechanism of action remained completely unknown. Natural components responsible for the pharmacological effects of *Cannabis sativa* were identified in the 1960s. Thereby, cannabidiol (CBD) was appointed first, followed by the lipophilic compound Δ^9-tetrahydrocannabinol (THC), which explained most of the psychoactive effects that *Cannabis sativa* has (Mechoulam, Shvo 1963, Gaoni, Mechoulam 1964, Grunfeld, Edery 1969).

Because of its strong hydrophobic characteristics, THC's mechanism of action was thought to be general perturbation of the cellular membranes rather than binding a specific site. However, this hypothesis was proven wrong by the discovery that only a specific THC enantiomere has its effect. The pharmacological action was proven to be enantioselective and thus to contain a more specific sort of binding (Mechoulam et al. 1980, Mechoulam et al. 1988).

In 1988, binding sites specific for THC were found in the brain using radio labeled of THC (Devane et al. 1988). By screening the affinity of several previously cloned orphan G-protein-coupled-receptors (GPCR) for THC, a specific receptor was found and named CB_1. It was shown to be very abundant in the brain and thus suggested to be responsible for the psychoactive effects of THC. Another receptor, with a very different amino acid sequence, was also identified by its affinity for THC, named CB_2 and shown to be more present in immune cells (Devane et al. 1988, Matsuda et al. 1990, Munro, Thomas & Abu-Shaar 1993). Recently, pain reducing effects of cannabinoids were shown to be mediated by the glycine receptor rather than CB_1 (Xiong et al. 2011).

To reveal normal functioning of CB_1 and CB_2, endogenous ligands needed to be found. Among others, 2-arachidonoyl-glycerol (2-AG) and *N*-arachidonoylethanolamine (anandamide or AEA) have been found (Devane et al. 1992). Furthermore, their catabolic pathways have been studied thoroughly (De Petrocellis, Di Marzo 2009, Di Marzo 2009). Biosynthetic enzymes have recently been shown to play a fundamental role in both spatial and temporal aspects of endocannabinoid functioning (Di Marzo et al. 1994, Di Marzo et al. 1996, Di Marzo 2011).

Endocannabinoids suppress neurotransmission by retrograde signaling (Wilson, Nicoll 2001). They are produced by the postsynaptic cell and act on the presynaptic receptor (Di Marzo 2011). They are shown to induce both short and long-lasting reduction of neurotransmitter release. Fig. I.1 shows that cannabinoid receptors are present in multiple brain regions.
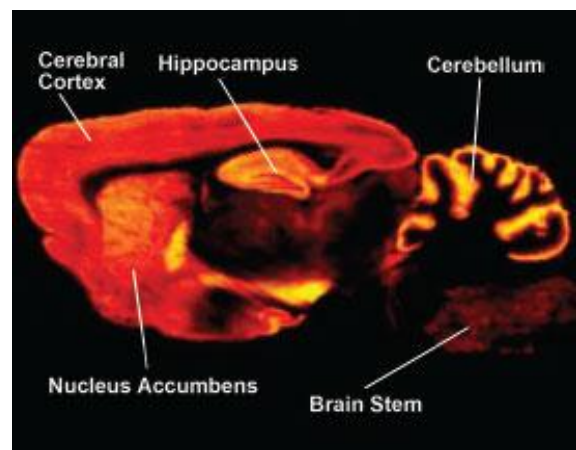

Figure I.1: Distribution of the Cannabinoid receptor in the rat brain. *Orange and yellow indicate high binding of radioactive CP-55,940, a CB_1 ligand. Cannabinoid receptors are present in the hippocampus, cerebellum, cerebral cortex, substantia nigra and nucleus accumbens (Herkenham).*

Agonism and antagonism of CB_1

Several synthetic cannabinoid receptor agonists have been developed since the early 1990s. Behavioral effects of these agonists were tested and included appetite stimulation. Therefore, these were prescribed to increase appetite in AIDS and cancer patients (Di Marzo et al. 2001, Mattes et al. 1994).

In 1994, the first potent, orally effective and CB_1 specific antagonist was found. SR141716A was shown to antagonize the pharmacological CB_1-mediated effects of both synthetic

agonists and the endogenous anandamide. SR141716A was shown to have a 1000-fold higher affinity for CB_1 than for the CB_2, which was mentioned to be useful for distinguishing CB_1 and CB_2 specific effects (Rinaldi-Carmona et al. 1994). SR141716A also showed reduction of appetite for sucrose and ethanol, by altering brain reward circuits (Kirkham 2005). Contrarily to prescription of CB_1 agonists to AIDS and cancer patients, appetite suppression was now realized by a CB_1 specific antagonist (Rinaldi-Carmona et al. 1994).

Despite the therapeutic effects of SR141716A (Rimonabant) in treatment of obesity, a 4.7 kg greater weight reduction per year compared to placebo, pleiotropic effects were noticed (Christensen et al. 2007). Rimonabant was shown to increase the risk of psychiatric adverse events, even if depressed mood was an exclusion criterion for treatment (Christensen et al. 2007). It was granted market authorization by the European Commission in June 2006. In January 2009, this market authorization was withdrawn. The Committee for Medicinal Products for Human Use noticed doubling in depression risk in July 2007. In June 2008, 5 suicides were related to Rimonabant in ongoing trials (Kwatra 2010).

However, antagonizing the endocannabinoid system as treatment of obesity is not rejected completely (Le Foll, Gorelick & Goldberg 2009). It is speculated that only specific sub-populations, for example based on their genetic profile, are at-risk (Kwatra 2010). Rimonabant might be given without the depressive and suicidal side effects if these individuals would be excluded from treatment (Kwatra 2010). Another option would be to modulate the endocannabinoid system by other means, for example, blocking catabolic enzymes (Di Marzo 2008; Le Foll, Gorelick & Goldberg 2009). Admitting an antagonist that acts only peripherally might also be an option.

The fourth option for preventing severe side effects might be to use a neutral antagonist instead of an inverse agonist. CB_1 is thought to have constitutive activity and Rimonabant is thought to operate as an inverse agonist. The blockage of constitutive activity is suggested to cause the adverse effects (Pertwee 2005).

Activation of different G-proteins by different CB_1 ligands

Next to inverse agonism, ligand specificity in activation of distinct G-proteins and intracellular transduction pathways is an interesting property of CB_1. The intracellular palette of G-proteins and other transduction molecules differs per cell type. Ligands have been shown to activate certain pathways more intense than to others. Antagonists might also possess this specificity, which might have many implications for treatment with a CB_1 antagonist. Namely, CB_1 antagonism could be cell type specific.

Stimulation of transmitter release through CB_1 on astrocytes

Endocannabinoids have recently been shown to mediate neuron-astrocyte communication (Navarrete, Araque 2008). Neuron-neuron endocannabinoid signaling leads to suppression of transmitter release, for example causing depolarization induced suppression of excitation (DSE). In contrast, stimulation of CB_1 on astrocytes causes endocannabinoid mediated synaptic potentiation (eSP) (Navarrete, Araque 2010). Ca^{2+} elevation in the astrocyte by activation of CB_1 causes increased release of glutamate, leading to eSP.

Prospects for antagonizing CB_1

These new data suggest that interfering CB_1 with neutral antagonists or inverse agonists causes both a relative increase and decrease of excitatory neurotransmitter release. Even more interestingly it is that these pathways could be separated pharmacologically. Namely, there is a difference between activated G-proteins in these two pathways. Since activation of intracellular pathways is in general ligand specific, the two pathways might also be antagonized differentially.

Together with the concept of neutral antagonism, this could be of high value for finding an effective drug with less adverse effects.

Chapter 1: Presence of endocannabinoids

Generation and degradation of endocannabinoids

To understand both proper functioning and pharmacological intervention of CB_1, it is important to understand the role and characteristics of its endogenous ligands and enzymes involved in biosynthesis and catabolism of these ligands. Multiple pathways of inducing endocannabinoid signaling have been found (Edwards, Kim & Alger 2006). Evidence for storage of endocannabinoids in vesicles is lacking, suggesting that release of endocannabinoids is directly mediated by biosynthesis rather than by release out of earlier filled vesicles (Di Marzo 2008). Activation of metabolic and catabolic biosynthetic pathways thus is the key in determining endocannabinoid signaling.

Presence of Anandamide

Anandamide is formed out of *N*-arachidonoyl-phosphatidylethanolamines (NArPE), a small family of membrane phospholipids. This is shown in fig. 2.1. The precise route of conversion from *N*-arachidonoyl-phosphatidylethanolamines to anandamide is controversial and multiple pathways are suggested to occur in brain homogenates (Di Marzo 2011)(Di Marzo 2008).

Deactivation of endocannabinoids might be as important as their production. In rodents, inactivation of anandamide is achieved by fatty acid amino hydroxylase (FAAH) (Starowicz, Nigam & Di Marzo 2007). Anandamide is degraded by FAAH into arachidonate and ethanolamine and into prostamide endoperoxide by cyclooxygenase 2 (Di Marzo 2011).
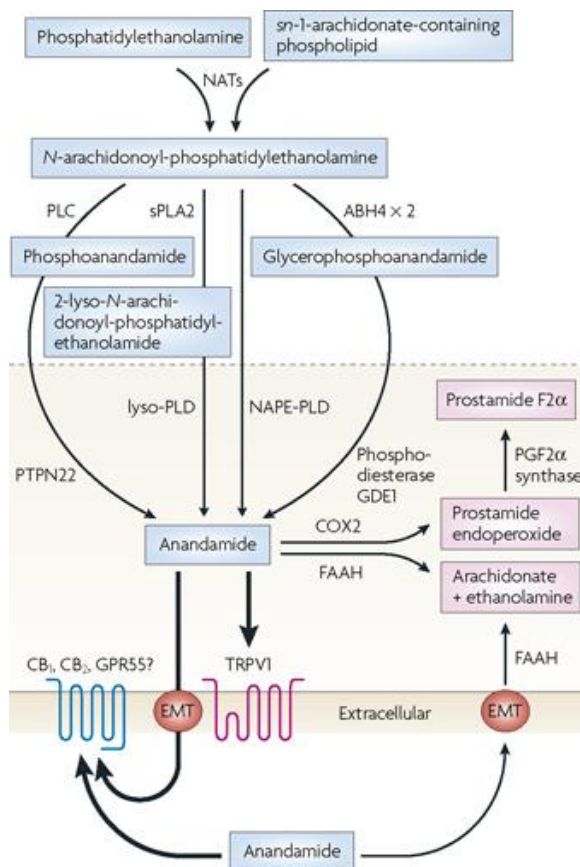
ABH4	αβ-hydrolase 4
CB$_{1/2}$	cannabinoid receptor ½
COX2	cyclooxygenase 2
EMT	endocannabinoid membrane transporter
FAAH	fatty acid amide hydrolase
GDE1	glycerophosphodiester phosphodiesterase 1
GPR55	G protein-coupled receptor 55
NAPE-PLD	*N*-acyl-phosphatidylethanolamine-selective phosphodiesterase
NATs	*N*-acyltransferases
sPLA2	soluble phospholipase A2
PLC	phospholipase C
PLD	phospholipase D
PTPN22	protein tyrosine phosphatase, non-receptor type 22
TRPV1	transient receptor potential, vanilloid subtype 1 receptor

Figure 1.1: Biosynthesis of anandamide. *The biosynthetic pathways for anandamide are shown in blue, degrading pathways are shown in pink. Thick arrows note movement or action. Abbreviations of are explained in the box on the right. (Di Marzo 2008).*

Presence of 2-AG

The direct precursor for 2-AG is *sn*-1-acyl-2-arachidonoylglycerols (AArG), which is mainly produced out of phosphatidylinositol by phospholipase Cβ (PLCβ). AArG is converted to 2-AG by *sn*-1-diacylglycerol lipase α and β (DAGLα and DAGLβ) (Bisogno et al. 2003). Fig. 1.2 shows the biosynthesis more in detail. Activation of biosynthetic pathways is triggered by elevations of Ca^{2+}. In case of 2-AG, biosynthetic enzymes, including phospholipase Cβ (PLCβ) and diacylglycerol lipase-α (DAGLα), are located on the membrane between the dendrite and the soma, near metabotropic receptors. Ca^{2+} concentration can be elevated by either activation of postsynaptic metabotropic receptors, or postsynaptic depolarization induced influx of Ca^{2+} which will be shown in chapter 2 (Di Marzo 2011).

Presence of endocannabinoids

It can be concluded that endocannabinoids are present in the brain, depending on biosynthesis and degradation. Anandamide and 2-AG have been studied most thoroughly, but more endogenous substances are known. The presence of endocannabinoids is a key-step in the functioning of CB_1. Now this is known, the next chapter will focus on the actual effects that are mediated by endocannabinoids.

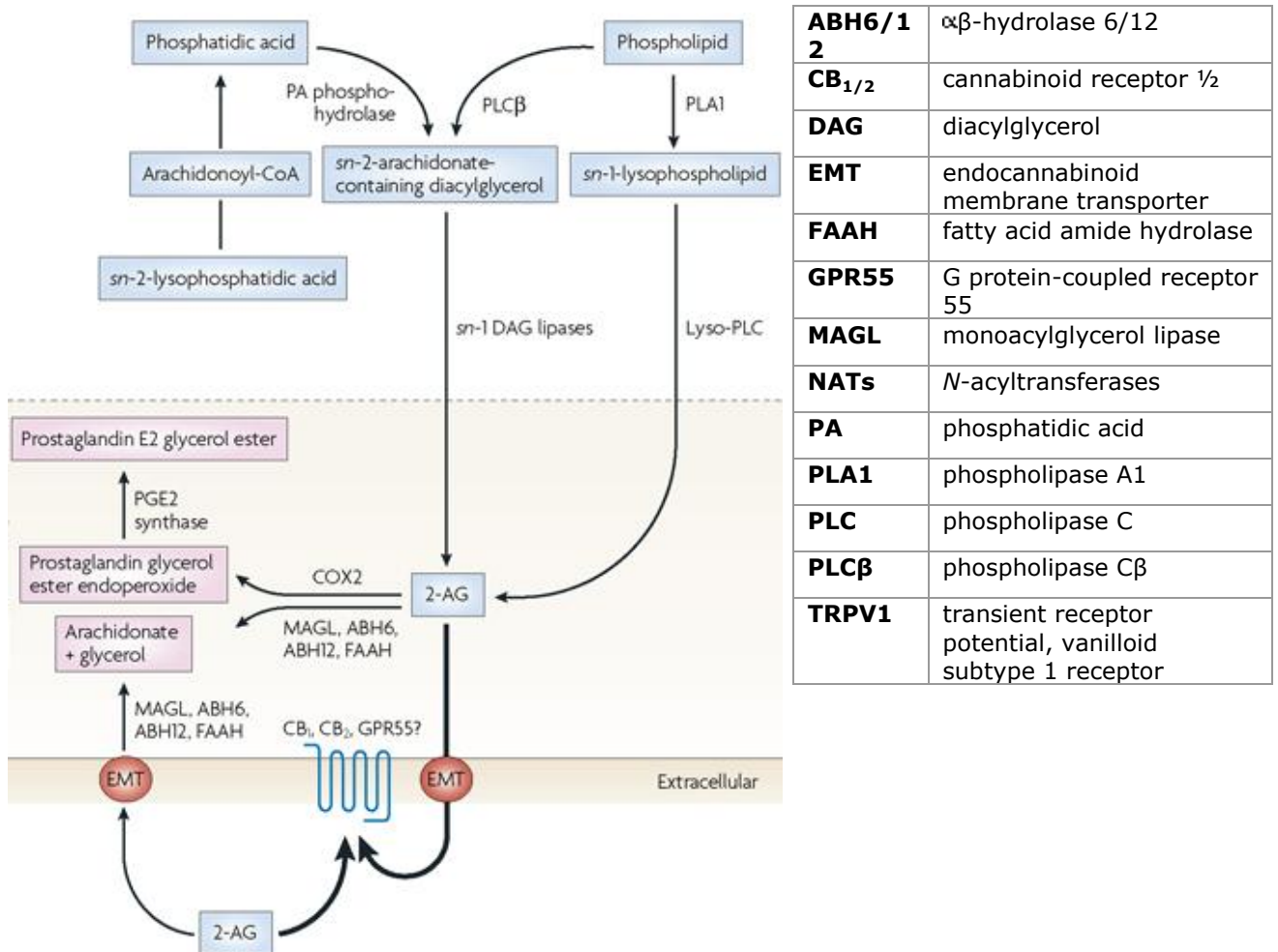| ABH6/12	αβ-hydrolase 6/12
$CB_{1/2}$	cannabinoid receptor ½
DAG	diacylglycerol
EMT	endocannabinoid membrane transporter
FAAH	fatty acid amide hydrolase
GPR55	G protein-coupled receptor 55
MAGL	monoacylglycerol lipase
NATs	*N*-acyltransferases
PA	phosphatidic acid
PLA1	phospholipase A1
PLC	phospholipase C
PLCβ	phospholipase Cβ
TRPV1	transient receptor potential, vanilloid subtype 1 receptor

Figure 1.2: Biosynthesis of 2-AG. The biosynthetic pathways for 2-AG are shown in blue, degrading pathways are shown in pink. Thick arrows note movement or action. Abbreviations are explained in the box on the left. (Di Marzo 2008).

Chapter 2: Electrophysiological effects of endocannabinoids

Multiple electrophysiological effects of endocannabinoids have been found since the beginning of the 21st century. Understanding these different effects and their underlying pathways is crucial for understanding functioning of CB_1.

Depolarization induced Suppression of Inhibition (DSI)

Depolarization of postsynaptic neurons has been shown to induce suppression of the release of inhibitory neurotransmitters by the presynaptic neuron. Endocannabinoids were shown to mediate this depolarization induced suppression of inhibition (DSI), thereby functioning as retrograde messengers (Wilson, Nicoll 2001).

In transverse hippocampal slices of 300μm, IPSC's were generated in or near the CA1 *stratum pyramidale* using electrodes. DSI was tested as follows. 30 stimuli were given, at 0.33 Hz. After 8 stimuli, postsynaptic depolarization from -60 mV to 0mV was induced for 5 seconds. DSI was defined as the relative decrease of evoked IPSCs (eIPSCs), comparing the average of the three eIPSCs just before depolarization ($amp_{baseline}$) with the three eIPSCs just after the depolarization (amp_{test}) (Wilson, Nicoll 2001). DSI can be defined by the following formula: DSI (%) = $100(1-(amp_{test}/amp_{baseline}))$.

DSI was proven to require endocannabinoids as shown in fig. 2.1. Slices that were pre-incubated with AM251 or SR141716, both CB_1 selective antagonists, showed a decrease in DSI from 30% in control to about 5% (Wilson, Nicoll 2001). Furthermore, fig. 2.1 shows that this effect lasts for about 20 seconds.

Depolarization induced suppression of GABA release has thereby been shown to be mediated by intracellular Ca^{2+} elevations in the postsynaptic cell. Namely, DSI was shown to be blocked in presence of BAPTA, a fast Ca^{2+} buffer. Furthermore, depolarization was ineffective when extracellular Ca^{2+}-influx was blocked by perfusion of the neurons in a Ca^{2+}-free solution (Ohno-Shosaku, Maejima & Kano 2001). Endocannabinoid signaling is thus activated by depolarization and depends on calcium influx. Activation of this pathway causes
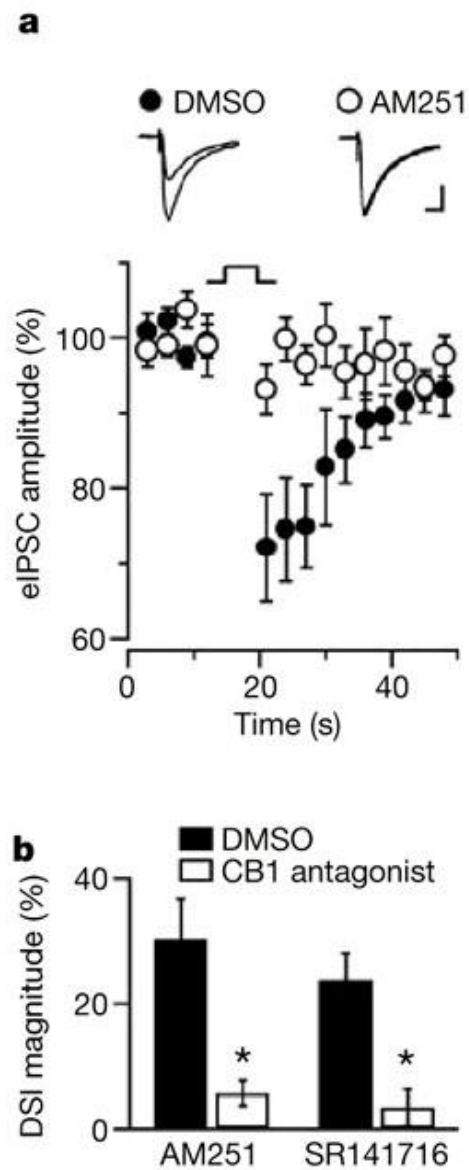
suppression of synaptic inhibition. See fig. 2.7.

***Figure 2.1: Depolarization induced Suppression of Inhibition (DSI) requires endogenous cannabinoids in hippocampal neurons.** a) In pyramidal neurons, neural depolarization causes suppression of evoked IPSCs amplitude in DMSO controls (n=10). This effect was suppressed by AM251, a CB_1 antagonist. b) The effect on DSI magnitude was undone in slices that were pre-incubated in AM251 (n=11), or SR141716 (n=11), both CB_1 antagonists. An * indicates that P < 0.005 (Wilson, Nicoll 2001).*

Endocannabinoids are thereby shown to act presynaptic and function as retrograde messengers. Namely, synaptic response to the release of neurotransmitter from a single vesicle (quantal size) of miniature GABA-induced events (mIPSCs) is not affected as well as the sensitivity of postsynaptic membrane in case of iontophoresion (Wilson, Nicoll 2001).

Anandamide, 2-AG and other endocannabinoids are lipid transmitters and thus poorly soluble. After release by the postsynaptic cell, these agonists are thought to stick in the extra cellular matrix and thus act only nearby (Devane et al. 1992, Di Marzo 2008). Usually endocannabinoids are effective within 20 µm of the synapse by whose activity they are produced. However, signaling can be both homosynaptic and heterosynaptic (Di Marzo 2011).

Since 2001, the role of endocannabinoids in DSI has not only been shown in hippocampal neurons, but in other brain regions as well (Kano et al. 2009).

Depolarization induced Suppression of Excitation (DSE)

In addition to transient inhibition of neurotransmitter release at inhibitory synapses, reduction in release of neurotransmitters has also been found in excitatory synapses, in the cerebellum (Kreitzer, Regehr 2001). Endocannabinoids mediate decrease in excitatory postsynaptic currents (EPSCs). The mechanism of depolarization induced suppression of excitation (DSE) is shown to be quite like DSI, except the properties of the finally decreased neurotransmitter. DSE can be defined by the following formula: DSE (%) = $100(1-(amp_{test}/amp_{baseline}))$. Thereby, it was found to be small in the first second following postsynaptic depolarization, approach a maximum between 5 and 10 seconds, which decays with a $t_{1/2}$ of 15 to 20 seconds (Kreitzer, Regehr 2001).

At excitatory synapses that project onto Purkinje cells, depolarization decreases the amplitude of EPSCs. Endocannabinoids are shown to decrease presynaptic calcium influx. Release of these endocannabinoids is caused by postsynaptic calcium influx elevations. Postsynaptic calcium buffering by BAPTA namely blocks decrease of presynaptic calcium influx as well as amplitude of EPSCs. AM251, a CB_1 antagonist is shown to prevent DSE, agonist WIN occludes DSE (Kreitzer, Regehr 2001). This decrease in EPSC amplitude by decrease of excitatory neurotransmitter release has been shown in neurons other than Purkinje cells as well (Kano et al. 2009).

Endocannabinoid mediated short-term depression (eCB-STD)

Where DSI and DSE are induced by postsynaptic increase of calcium influx, endocannabinoid mediated short-term depression (eCB STD) is defined as the electrophysiological effect of endocannabinoids through activation of postsynaptic group I metabotropic glutamate receptors (mGluRs), lasting for several minutes.

Amplitude of EPSCs at cerebellar Purkinje cells and eIPSCs at CA1 pyramidal cells have been shown to be decreased by mGluR mediated release of endocannabinoids (Maejima et al. 2001, Varma et al. 2001). Group I mGluR can be agonized by DHPG. Fig. 2.2 shows that both depolarization and DHPG induce depression. However, DHPG induces an effect that does not depend on postsynaptic calcium increase and lasts much longer, namely several minutes. Both effects however were blocked by SR 141716 A.

eCB STD enhances the effect of DSE on EPSCs by group I mGluRs and vice-versa. However, the two pathways are distinct. Group I mGluRs are not necessary for DSE and retrograde signaling by endocannabinoid can be produced by a Ca^{2+} dependent pathway as well as in abstinence of postsynaptic Ca^{2+} (Maejima et al. 2001). The latter was shown by intracellular addition of BAPTA. Increase of Paired Pulse Ratio (PPR), suggests presynaptic effect, indicating an increase in calcium concentration.

eCB STD is shown in many other brain regions as well and endocannabinoid functioning mediated by mGluRs is thought to be more important compared to depolarization induced suppression of transmitter release(Kano et al. 2009).
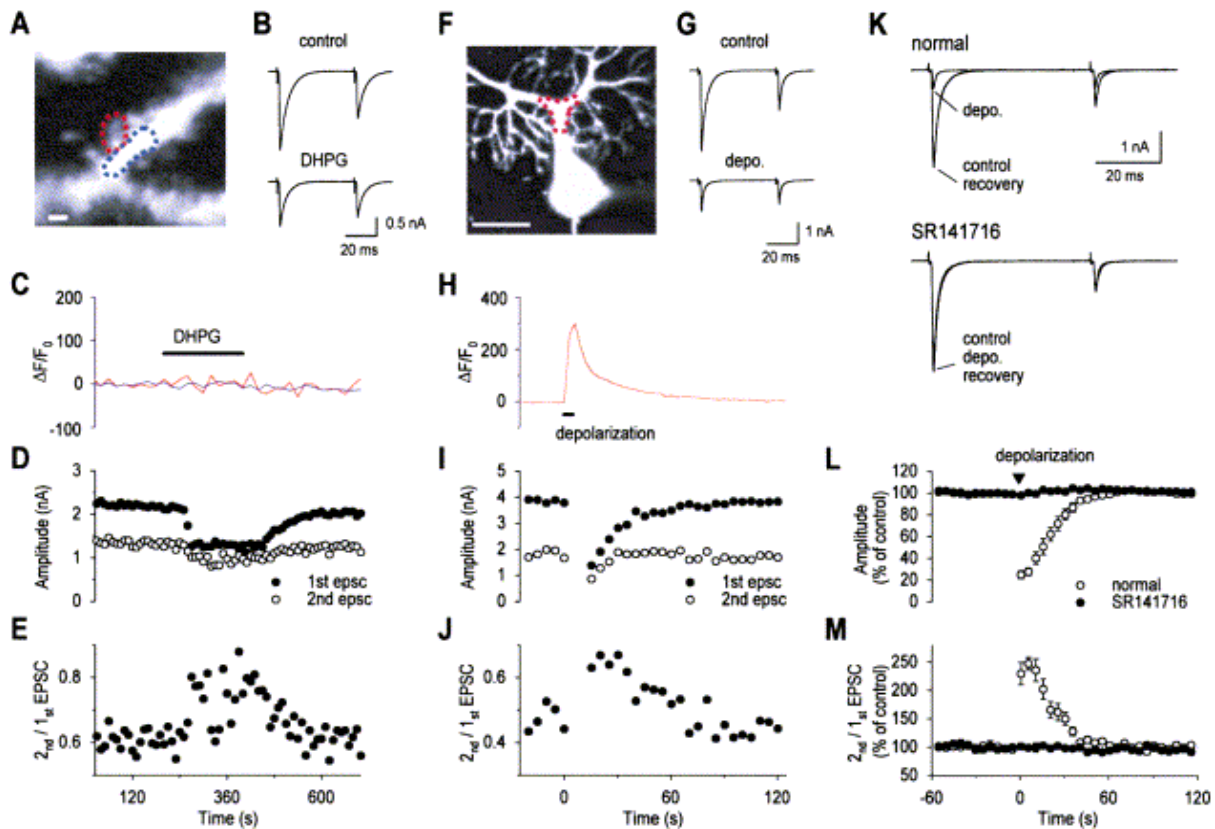
Figure 2.2: Depression of Climbing fiber-EPSCs by DHPG and Depolarization.
(A−E) In Purkinje cells (PC), activation of group I GluR by DHPG induces depression of EPSCs, which does not require elevation of $[Ca^{2+}]_i$. Depression of CF-EPSCs is caused (B and D), lasting for a couple of minutes, accompanied by increase in the paired-pulse ratio, indicating a presynaptic effect(E). Bath-applied DHPG (50 µM) causes no change in $[Ca^{2+}]_i$ (C).
(F−J) Direct depolarization of PC (five depolarizing pulses with 100 ms duration to 0mV from −80mV, repeated at 1 Hz) cause transient elevation of $[Ca^{2+}]_i$ in PC dendrites ([H], measured in the area shown in [F]). It causes a transient depression of CF-EPSCs, lasting for a shorter period of time (G and I) and is also accompanied by significant increase in the paired-pulse ratio (J).
(K−M) Application of SR141716, a CB_1 antagonist, totally abolishes the depolarization-induced transient depression of CF-EPSCs. Records in normal saline and those in SR141716 were obtained sequentially from the same PCs (Maejima et al. 2001).

Long term Depression (LTD)

Furthermore, endocannabinoids were shown to mediate long term depression (LTD), in which retrograde signaling is also involved. At cortico-striatal afferents LTD was caused in the striatum using high-frequency stimulation (HFS) of 1 s duration at 100 Hz. At these neurons, this form of synaptic plasticity was shown to depend on activation of CB_1 (Gerdeman, Ronesi & Lovinger 2002). In both pharmacologically and genetically caused abstinence of CB_1, LTD was not present as can be seen in fig. 2.3 and 2.4. Thereby, LTD was facilitated by elevations of extracellular endocannabinoids concentrations by blocking their uptake. Since 2002, endocannabinoid induced LTD has been shown in many other brain regions as well (Kano et al. 2009).
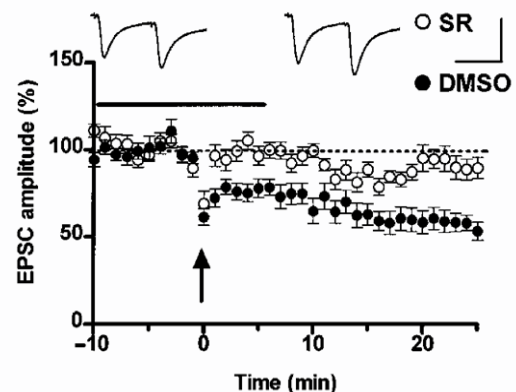

Figure 2.3: Induction of striatal LTD depends on CB1 receptor activation. *LTD was blocked in slices that were pre-incubated with the CB1 antagonist SR141716A, as compared with DMSO control. Dark bar indicates the treatment with SR or DMSO. (Gerdeman, Ronesi & Lovinger 2002)*
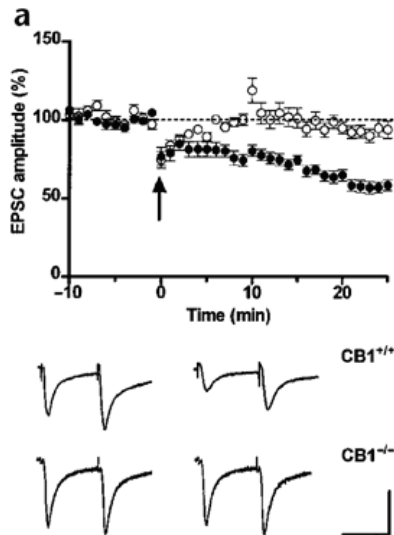
10

Figure 2.4: Striatal LTD is not seen in CB1⁻ᐟ⁻ mice. *High frequency stimulation (HFS) paired with postsynaptic depolarization (arrow) induced LTD after a stable baseline in $CB1^{+/+}$ (●) mice. This effect is not found in $CB1^{-/-}$ (○) mice. LTD was determined by EPSC's in medium spiny neurons. In $CB1^{+/+}$ EPSC amplitude was 60 ± 4% of the baseline amplitude (n = 10). In $CB1^{-/-}$ it was 95 ±7% baseline (n = 10). At the bottom, 10-trace averages of paired EPSCs from a striatal neuron before (left) and after (right) HFS are shown. The effect was not found in absence of CB_1 (Gerdeman, Ronesi & Lovinger 2002).*

Endocannabinoids potentiate release through CB_1 on astrocytes.

In contrast to *suppression* of presynaptic neurotransmitter release, endocannabinoids have recently also been shown to *potentiate* neurotransmitter release. In hippocampal CA3 – CA1 synapses, depolarization was shown to induce elevations in Ca^{2+} concentrations in atrocytes, which causes potentiation of synaptic transmission (Navarrete, Araque 2010).

This effect was measured at *a fraction* of neurons in hippocampal slices, using paired recording and is shown in fig. 2.5. It was induced by a postsynaptic neural depolarization to 0 mV for 5 seconds (green cell). EPCSs were evoked by minimal presynaptic stimulation. Neural depolarization was shown to cause an increase in mean amplitude of EPSCs and increased probability of neurotransmitter release. This effect was abolished by the CB_1 antagonist AM251 and also absent in CB_1 knockout mice, indicating the involvement of CB_1 and

endocannabinoids. This effect was named endocannabinoid mediated synaptic potentiation (eSP).

Furthermore, the effect was also shown to be absent when the depolarized neuron (green), was loaded with BAPTA-loaded, which prevents release of endocannabinoids. This suggests postsynaptic release of endocannabinoids. Thereby, synaptic potency, the mean EPSC amplitude excluding failures, remained constant and Paired pulse ratio was increased, suggesting a presynaptic effect.

Already in 2008, hippocampal astrocytes were shown to express functional CB_1, stimulating the release of glutamate, leading to increase of synaptic excitability due to activation of neuronal NMDA receptors (Navarrete, Araque 2008). The electrophysiological effect of postsynaptic depolarization was shown to depend on this earlier described pathway. The postsynaptic produced endocannabinoids act on CB_1 receptors of astrocytes and thereby induce Ca^{2+} elevations. This elevation causes release of glutamate, acting on neurons to increase excitability (Navarrete, Araque 2010). It is important to mention that eSP is not the only electrophysiological action that can be measured. DSE, caused by endocannabinoids directly acting on CB_1 of presynaptic neurons, also takes place at these hippocampal CA3 – CA1 synapses (Navarrete, Araque 2010). See fig. 2.6.

Both the depolarized postsynaptic neuron (green) and non-depolarized postsynaptic neuron (blue) can be activated by presynaptic stimulation. These synapses are respectively homoneuronal and heteroneuronal, referring to the depolarized postsynaptic neuron. In heteroneuronal synapses both DSE and e-SP can be found, in homoneuronal synapses only DSE (Di Marzo 2011).

Usually, endocannabinoids act locally (Di Marzo 2011). DSE is shown to occur close-by the depolarized neuron, while eSP occurs at greater distance. The effect by astrocytes is able to cover a greater distance than direct acting on the presynaptic neuron. Signaling within astrocytes is able to cover relative great distance.
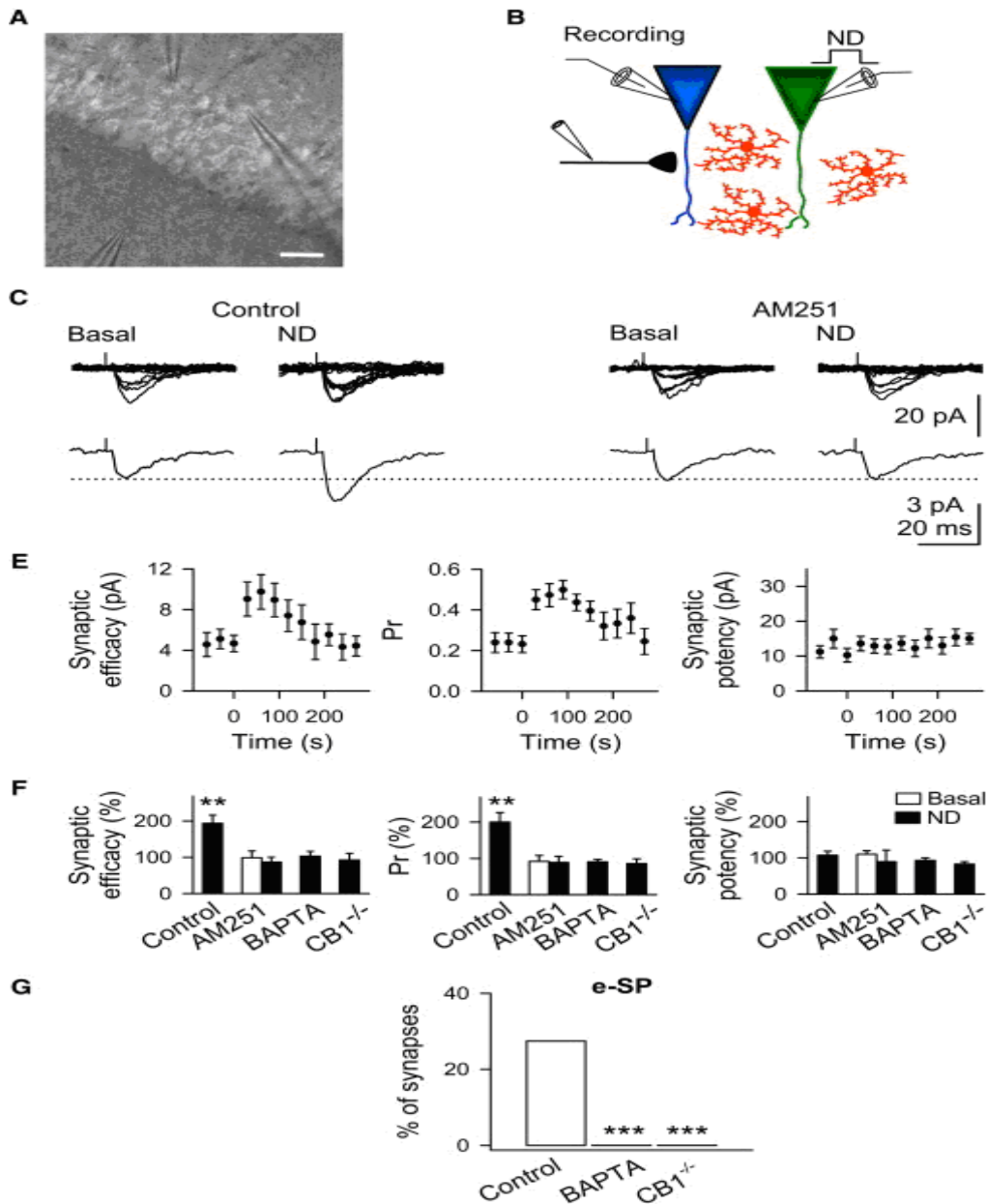
Figure 2.5: Endocannabinoids potentiate transmitter release at hippocampal pyramidal CA3-CA1 synapses. *At a fraction of CA-1 neurons, potentiation was found, in contrast to the less controversial depression of transmitter release. This figure focuses on the neurones that showed endocannabinoid mediated synaptic potentiation (e-SP) (Navarrete, Araque 2010).*

*(**A** and **B**) The blue and green CA-1 neurons are both postsynaptic cells. The green neuron was depolarized (ND). The black neuron was stimulated by an electrode at the minimal level to evoke EPSCs. Red cells are astrocytes. EPCSs were measured by the electrodes in both the blue and green cells (Navarrete, Araque 2010). The picture shows these paired recorded CA1 pyramidal neurons and the stimulation electrode (bottom). The bar represents 40 µm.*

*(**C**) EPSC amplitude responses were measured of 20 consecutive stimuli. This includes failures of synaptic transmission. Top traces show individual amplitudes, down traces averaged EPSCs. This was done before and after ND both in presence and absence of AM251, a CB_1 agonist. In absence of AM251, potentiation is tackled.*

*(**E** and **F**) Synaptic efficacy is defined as the mean amplitude of responses including successes and failures of neurotransmission. Pr is the probability of neurotransmitter release. Synaptic potency was measured as mean EPSC amplitude excluding failures. These three values were each relatively compared for AM251, BAPTA and $CB_1^{-/-}$ in (F). Increase of synaptic efficiency was tackled by AM251, indicating CB_1 involvement. This was confirmed by $CB_1^{-/-}$. BAPTA indicated Ca^{2+} dependency.*

*(**G**) As mentioned, only a proportion of synapses showed e-SP after ND. The disastrous effects and thus importance of BAPTA and $CB_1^{-/-}$ on this fraction, is shown here.*

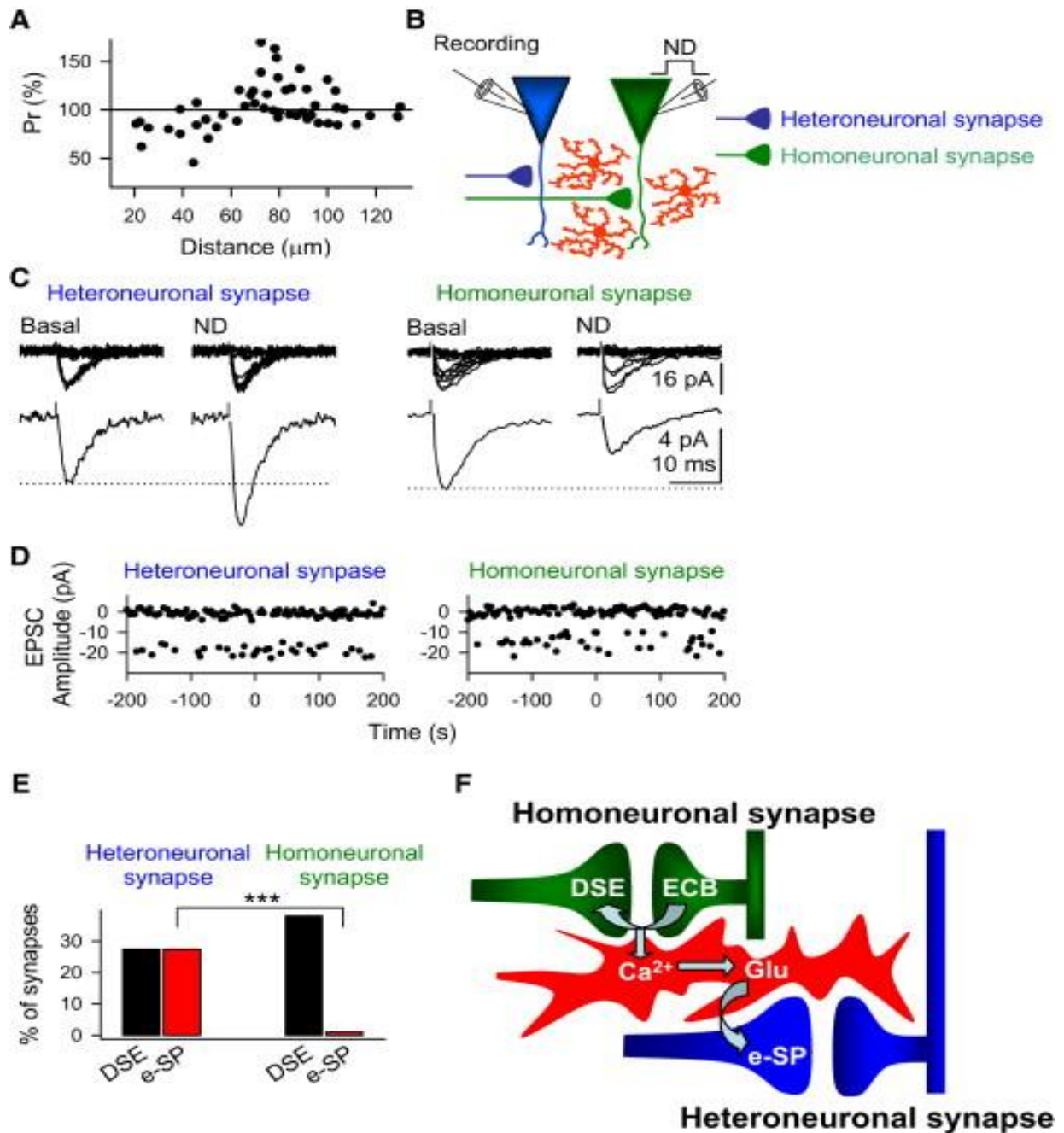***Figure 2.6: Endocannabinoids induce homoneuronal synaptic depression and heteroneuronal synaptic potentiation.***

*(**A** and **B**) Paired recordings were performed, in basal conditions and while the green neuron was depolarised. Stimulation was given either heteroneuronal synaptic (onto the blue postsynaptic cell) or homoneuronal synaptic (onto the green recorded postsynaptic cell).*

*(**C**) EPSC's amplitude were measured individually (top traces) and the mean was calculated (bottom traces). When the stimulation was given heteroneuronal synaptic relative to the depolarized (ND) cell, average amplitude shows an increase. For the homoneuronal synapse, stimulation lead to decrease of neurotransmitter release. ND correlates with time 0.*

*(**D**) EPSC amplitudes were simultaneously recorded at heteroneuronal and homoneuronal synapses. Beginning of ND, given to the green cell, corresponds with time 0.*

*(**E** and **F**) Proportion of heteroneuronal and homoneruonal synapses that showed DSE and e-SP after ND was determined. The ND was given to the green cell at the top middle of F. Homoneuronal synapses only show DSE. In heteroneuronal synapses both e-SP and DSE occur. The first by direct effect of endocannabinoids (ECB), the latter by ECB, calcium driven glutamate release by astrocytes. (**A**) A correlation between the length between the stimulation electrode and the ND cell seems positively correlated with neuronal potentiation instead of suppression. (Navarrete, Araque 2010)*

Endocannabinoids mediate multiple electrophysiological effects

Endocannabinoids have been shown to mediate multiple electrophysiological effects. Depolarization induced suppression of inhibition (DSI) and excitation (DSE) share suppressed release of neurotransmitter, lasting several seconds. Both were shown in multiple brain regions. Another effect was measured to last for minutes and was named endocannabinoid mediated short-term depression (eCB-STD). The difference in timespan is explained by the postsynaptic receptor initiating endocannabinoid synthesis, channel linked R and mGlu1 R respectively. This is shown in figure 2.7. Longterm potentiation (LTD) is shown to be mediated by endocannabinoids as well, an effect lasting for tens of minutes. Incompatible with the classic paradigm of neuronal signaling, astrocytes were shown to be involved in endocannabinoid signaling. In contrast to the suppression of transmitter release as in neurons, endocannabinoids were shown increase the release of neurotransmitter in this case. Endocannabinoids were shown to potentiate synaptic transmission by activating CB_1 (eSP). Indeed, both DSI and eSP have a net effect of increasing excitability while DSE mediates the opposite. However, it looks more promising to distinguish between presynaptic suppression and increase of transmitter release. Sharing their dependency on activation of CB_1, they seem to be activated by complete distinct pathways. The different downstream pathways of CB_1 and their differential activation will now be discussed in the next chapter.
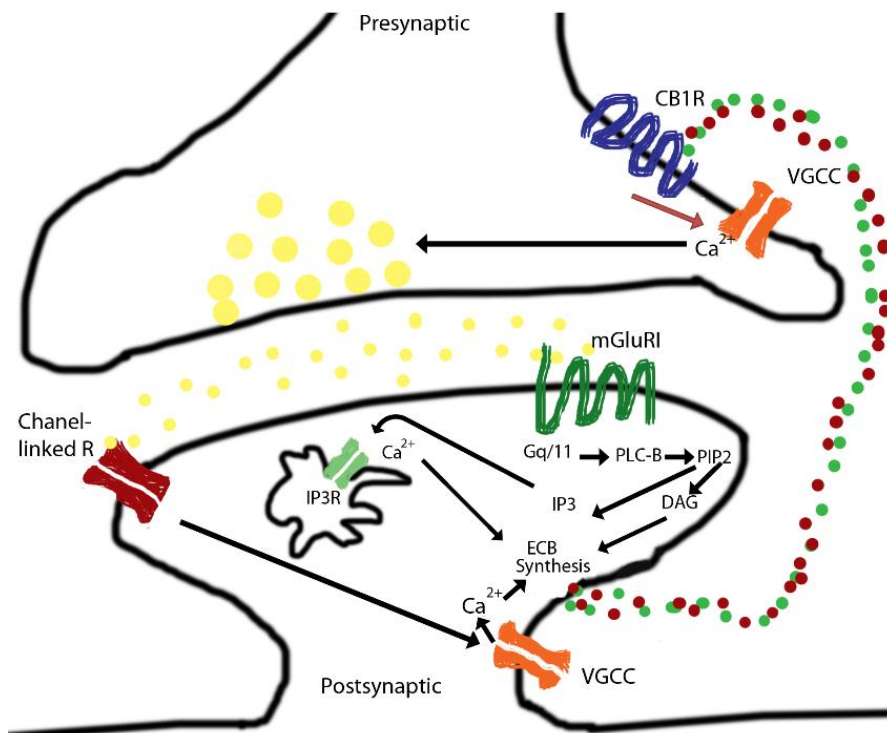

Figure 2.7: Production of endocannabinoids; differences between DSI/DSE and eCB-STD. *Released transmitter (yellow) can act on channel linked receptors, causing depolarization induced production of endocannabinoids. This is the case in depolarization induced suppression of both inhibition and excitation. Furthermore, released transmitter can act on type I mGluR's, inducing eCB-STD. DSE and DSI are indicated by the red pathway. Endocannabinoid mediated short term depression (eCB-STD) is shown by the green colors. Black arrows indicate activation, the red inhibition. eCB-STD is caused by a signal transduction pathway including $G_{q/11}$proteins which activate PLC-B. PLC-B hydrolyses PIP-2, splitting it into IP_3 and DAG. Gene activation by $G_{q/11}$ possibly explains the relative long effect of eCB-STD. NB. The generated endocannabinoids (red and green dots) are not different. They act via CB_1 to suppress presynaptic Ca^{2+} influx.*

CB_1 is a G-protein coupled receptor (GPCR), able to activate multiple intracellular signaling pathways and thereby to cause multiple physiological effects, including the electrophysiological effects described in chapter 2. See fig. 3.1. (Varga et al. 2008), Activated pathways are shown to enclose G-protein-independent signaling, receptor regulated events and multiple G-protein dependent signaling routes. Activation of the latter is shown to have ligand specificity (Hudson, Hebert & Kelly 2010). GPCR properties of CB_1 are important to understand this ligand specific signaling. Even more important these specificities might be for understanding the role of CB_1 in ligand specific physiological effects. Activation of CB_1 primarily causes $G_{i/o}$-protein activation, which leads to (1) inhibition of voltage-gated Ca^{2+} channels (VGCC), (2) activation of G-protein regulated inwardly rectifying K^+ channels (GIRK), (3) inhibition of formation of cyclic adenosine monophosphate (cAMP) and (4) activation of mitogen-activated protein kinases (MAPK) extracellular signal-related kinase (ERK)(Varga et al. 2008)(Lovinger 2008). G_s and $G_{q/11}$ are also activated by CB_1, activating adenylyl cyclise and increasing intracellular Ca^{2+}concentrations, respectively (Varga et al. 2008).
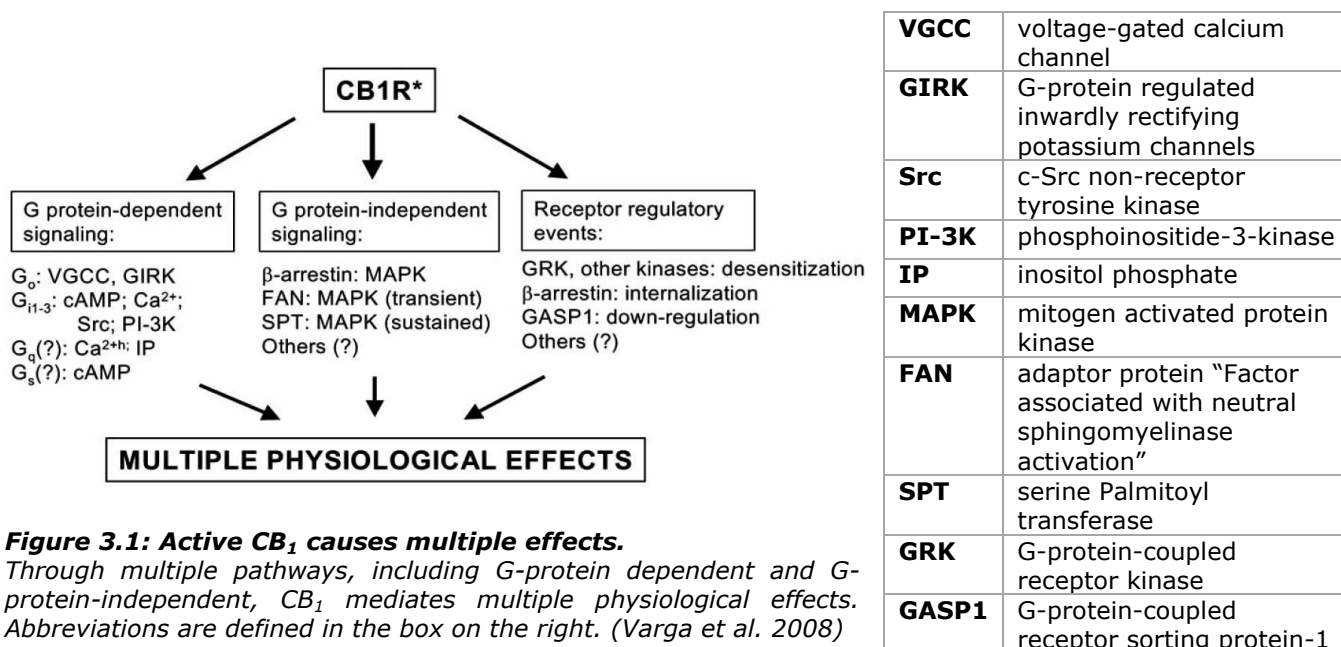

Figure 3.1: Active CB₁ causes multiple effects.
Through multiple pathways, including G-protein dependent and G-protein-independent, CB₁ mediates multiple physiological effects. Abbreviations are defined in the box on the right. (Varga et al. 2008)

VGCC	voltage-gated calcium channel
GIRK	G-protein regulated inwardly rectifying potassium channels
Src	c-Src non-receptor tyrosine kinase
PI-3K	phosphoinositide-3-kinase
IP	inositol phosphate
MAPK	mitogen activated protein kinase
FAN	adaptor protein "Factor associated with neutral sphingomyelinase activation"
SPT	serine Palmitoyl transferase
GRK	G-protein-coupled receptor kinase
GASP1	G-protein-coupled receptor sorting protein-1

$G_{i/o}$ mediates inhibition of voltage dependent Ca^{2+}-channels

The CB_1 antagonists anandamide, WIN 55,212-2 and CP 55,940 have been shown to inhibit N-type voltage gated calcium channels in cultured NG108-15 cells(Varga et al. 2008). These cells are hybrids of rat neuroblastoma and mouse glioma.This inhibition leads to a decrease in Ca^{2+} influx and can be blocked by pertussis toxin (PTX), showing its mediation by $G_{i/o}$. Furthermore, cAMP pathways were shown not to be involved in this effect (Varga et al. 2008).

Comparable research is performed in many other cell types, cultured neurons and brain slices. See table 3.1. This research includes both cells that endogenously express CB_1 and cells that were transfected with CB_1. Specific types of voltage-gated calcium channels were found to be blocked, using VGCC specific blockers. N-type, P/Q-type, L-type are antagonised by ω-conotoxin, ω-agatoxin and 1,4-dihydropyridine respectively (Demuth, Molleman 2006b).

It should be mentioned that endocannabinoids are also thought to have a direct, non CB_1 mediated, effect on Ca^{2+} channels. Ca^{2+} currents can be inhibited by micro molar concentrations of WIN 55,212-2. This inhibition could not be reversed by the CB_1 antagonist SR 141716A and was also achieved by the

usually inactive isoform of WIN 55,212-2, namely WIN 55,212-3.

Except this speculated direct effect on VGCC, inhibition of VGCC was only found mediated by activation of only one G-protein, namely activation of $G_{i/o}$.

$G_{i/q}$-dependent and independent mediation of intracellular [Ca^{2+}]

Intracellular calcium concentration was temporarily increased by 2-AG and WIN 55,212-2 in cultured NG108-15 cells. This effect was shown to be PTX sensitive and to rely on PLC mediated activation of IP3. IP3 causes release of Ca^{2+} from internal stores, also in neurons. Increase of intracellular Ca^{2+} concentrations seems contradictory to suppression of neurotransmitter release and inhibition of VGCC. However, subcellular localization is suggested to solve this puzzle. Increased intracellular Ca^{2+} concentration is thought to activate calcium dependent K^+-channels, causing depolarization (Demuth, Molleman 2006a).

However, in recombinant HEK cells as well as human trabecular meshwork cells, WIN55,212-2 was shown able to increase intracellular Ca^{2+} after treatment with PTX. These recombinant HEK cells, derived from Human Embryonic Kidney, stably expressed CB_1 (Varga et al. 2008). Release of calcium via IP_3 sensitive stores was shown to be $G_{i/o}$ dependent as well as $G_{i/o}$ independent.

$G_{i/o}$ activates G-protein regulated inwardly rectifying K^+ channels

Inwardly rectifying K^+ channels facilitate inward K^+-current when membrane potential is negative to reversal potential. In case of hyperpolarization, inwardly rectifying K^+ channels can help to push the membrane potential back to its resting potential. WIN 55, 212-2 was found to activate inward current, which was found to rely on this inward rectifying K^+-current, by mediated by G-protein dependent inward rectifying K^+ channel (GIRK)(Demuth, Molleman 2006a).

Cells, region	Agonist	Tested sensitive for	Inhibited Channel
NG-108-15 cells	Anandamide, WIN 55,212-2, CP 55,940	PTX, ω-conotoxin	N-type
Rat superior cervical ganglion transfected with CB_1	WIN 55,212-2, CP 55,940	PTX, SR141716, ω-conotoxin	N-type
Rat striatal neurons	WIN 55,212-2	PTX, ω-conotoxin	N-type
AtT-20 pituitary tumor cells	Anandamide	PTX	Q-type
Rat cortical and cerebellar brain slices	Anandamide	PTX, SR141716	P/Q-type
Cultured rat hippocampal neurons	Anandamide, WIN 55,212-2, CP 55,940	PTX, SR141716	N- and P/Q- type
Rat cerebral arterial smooth muscle cell	WIN 55,212-2	PTX, SR141716, (1,4-dihydropyridine)	L-type
HEK-293 (transfected with CB_1), (CHO transfected with CB_1), NG108-15 (endogenous CB_1)	Anandamide, (not WIN55,212-2, CP55,940 and HU-210)	Not for PTX	G-protein-independent effect on T-type

Table 3.1: Inhibition of the multiple subtypes of VGCCs is mediated mainly by $G_{i/o}$-protein activation. *Inhibition of channels by agonists has been shown in many regions and for multiple channels. PTX sensitivity indicates involvement of $G_{I/O}$. (Demuth, Molleman 2006b).*

$G_{i/o}$ regulates outward K^+ current by phosphorylation of ion channels

In cultured hippocampal neurons, WIN 55,212-2 increases voltage dependent A-type outward K^+ current (I_A) but decreases voltage independent D-type outward K^+ (I_D) current. Both effects were sensitive for SR 141716 and PTX, indicating involvement of CB_1 and $G_{i/o}$-protein activation.

I_A was found to be deactivated by phosphorylation of the channel by PKA, while I_D is suggested to be activated by phosphorylation by PKA. In these cells, activation of CB_1 was shown to decrease cAMP/PKA. Therefore, increase of I_A by WIN 55,212-2 was successfully mimicked by inhibitors of PKA, for example IP-20. The same inhibitor decreased I_D activity. On the other hand, activation of PKA, by 8-Bromo-cAMP or forskolin, caused decrease of I_A and increase of I_D (Demuth, Molleman 2006b).

In hippocampal neurons, voltage dependent K^+-currents were identified (Mitterdorfer, Bean 2002). See fig. 3.2. Contributions of specific subtypes, including I_A and I_D are shown. Increase of I_A and decrease of I_D suggest higher peak amplitude, but lower amplitude during the current.
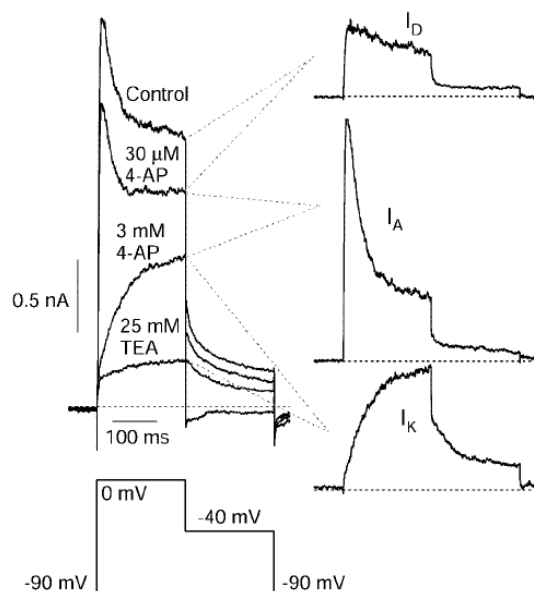

Figure 3.2: Pharmacological separation of I_A, I_D and I_K in individualized hippocampal pyramidal neurons. *Currents I_d, I_A and I_K were separated using blockers of the specific currents. These are high concentrations of 4-AP, low concentrations of 4-AP and TEA respectively (Mitterdorfer, Bean 2002).*

Direct activation of voltage dependent Na^+-channels by endocannabinoids

Both anandamide and WIN 55,212-2 are found to inhibit voltage-dependent Na^+-channels in mouse synaptosomes, isolated terminals of neurons (Nicholson et al. 2003). Neurotransmitter release induced by veratridine, including release of GABA and glutamate, was decreased by modulation of of Na^+-channels. Because CB_1 antagonist AM251 could not reverse this effect, it was suggested that endocannabinoids directly modulate voltage dependent Na^+-channels and thereby decrease release of both excitatory and inhibitory neurotransmitters (Nicholson et al. 2003).

CB_1 stimulates mitogen-activated protein kinases (MAPK)

CB_1 activation was also found to be involved in cell growth, transformations and apoptosis, by activation of mitogen-activated protein kinases (MAPK). Both G-protein dependent as well as G-protein independent pathways were found. G-protein dependent effects were found to be PTX sensitive, suggesting involvement of $G_{i/o}$(Varga et al. 2008). See fig. 3.1.

$G_{i/o}$, G_s and G_q regulate formation of cyclic adenosine monophosphate (cAMP)

Effects of CB_1 activated G-proteins was found to include both increase and decrease of cAMP, as shown in fig. 3.2. $G_{i/o}$, G_s, and G_q have all been showed to effect cAMP levels. Thereby, the differential palette of available adenylyl cyclase iso-enzymes determines which effect will take place. See fig. 3.3. Effects on cAMP are important for long-term changes in gene expression.

Presynaptic intracellular effects mediating DSE and DSI

Having knowledge of the multiple intracellular effects, in particular those on ion channels, the electrophysiological effects of endocannabinoids as mentioned in chapter 2 can be explained. The pathways involved in DSE and eSP will now be discussed.

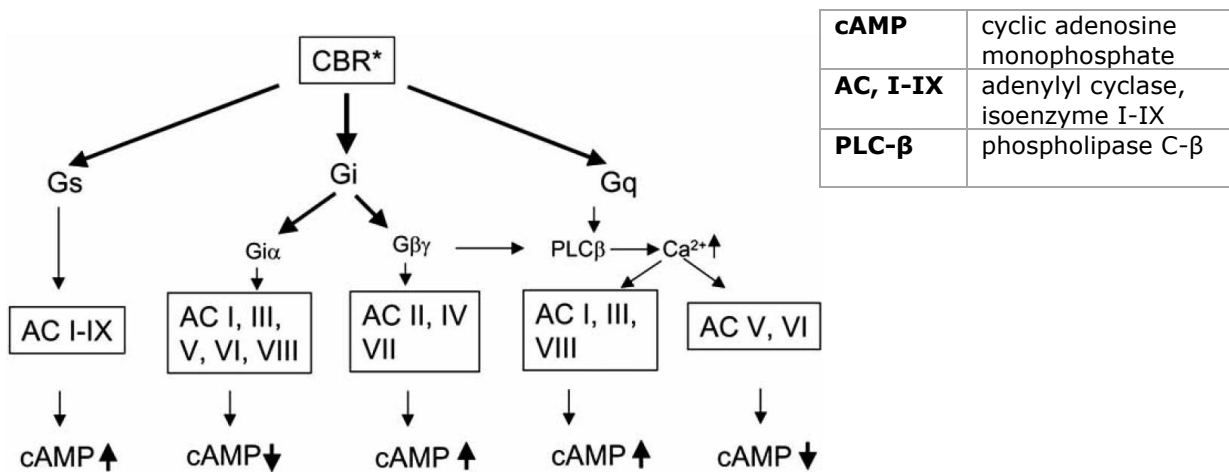In DSE, a decrease of calcium influx by VGCCs is thought to be

Figure 3.3: Active CB$_1$ regulates cAMP concentrations through multiple G-proteins. *Cellular background in adenylyl cyclase isoenzyme population, cellular G-protein profile and agonist specificity in G-protein activation reduces or increase cAMP concentrations (Varga et al. 2008).*

cAMP	cyclic adenosine monophosphate
AC, I-IX	adenylyl cyclase, isoenzyme I-IX
PLC-β	phospholipase C-β

responsible for the decrease in the release of excitatory neurotransmitter. After postsynaptic depolarisation, presynaptic calcium influx was shown to decrease, for about the same period of time as DSE lasts. This was found using fluo-4 dextran, a Ca^{2+} indicator that linearly responds to changes in presynaptic calcium. See fig. 3.4. Changes in calcium correlate with electrophysiological effects of DSE, which is small in the first second following postsynaptic depolarization, approach a maximum between 5 and 10 seconds and decays with a t$_{1/2}$ of 15 to 20 seconds (Kreitzer, Regehr 2001).

At the large presynaptic terminals at the calyx of Held, whole cell patch clamp measuring was performed. This experiment resulted in direct evidence for CB$_1$ induced decrease of presynaptic calcium current. Thereby, increase in membrane capacitance reflected Ca^{2+} dependent exocytosis. When WIN 55,212-2 was added, this increase was suppressed (Kushmerick et al. 2004). This indicates decrease in neurotransmitter release by decrease of Ca^{2+}.

More in general, is almost certainly that inhibition of VGCCs plays a role in presynaptic CB$_1$ actions, including both DSE and DSI (Lovinger 2008). In most cases this effect was found to depend on G$_{i/o}$ activation.
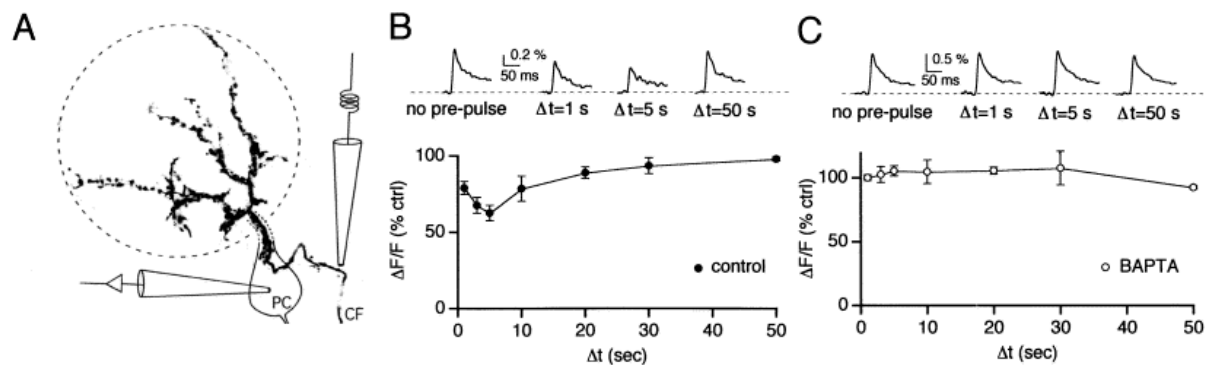

Figure 3.4: Postsynaptic depolarization inhibits presynaptic calcium influx. *Using fluo-4 dextran, Ca^{2+} was made visible and measured within the dotted circle. Climbing fibers (CF) were depolarized by voltage clamping in control conditions and at varying times following postsynaptic depolarization. EPCS's were measured at Purkinje cells (PC) in both control (B) and BAPTA addition (C). Calcium differences showed responsible for depolarization induced suppression of excitation, since deltaF/F correlates with suppression of EPSCs (Kreitzer, Regehr 2001).*

Presynaptic intracellular effects mediating e-SP in astrocytes

As mentioned in chapter 2, endocannabinoids potentiate synaptic transmission through a Ca^{2+} increase in astrocytes. Elevation of intracellular $[Ca^{2+}]$ in astrocytes is thought to cause release of glutamate, which acts on presynaptic mGluR, increasing transmitter release. eSP was shown to depend on Ca^{2+} elevations in astrocytes(Navarrete, Araque 2010). CB_1 was shown to be responsible for e-SP using AM251 and $CB^{-/-}$ knockouts, as shown in fig. 2.5. Therefore, eSP cannot be a direct, non-CB_1 mediated effect such as suggested for Ca^{2+} and voltage dependent Na^+ channels. Testing eSP in pre-treatment with PTX, it was shown to be mediated by $G_{i/o}$. Therefore, eSP is suggested to depend on activation of G_S or $G_{q/11}$ (Navarrete, Araque 2010).

Ca^{2+} elevation in a PTX insensitive way was also found in the earlier described cell cultures, including HEK cells and human trabecular meshwork cells. In that case, the Ca^{2+} elevation was shown to be caused by PLC mediated activation of IP3.

At homoneural synapses only DSE occurs, as shown in fig. 2.6. At heteroneural synapses, both DSE and e-SP are measured. Figure 3.5 shows the increase of e-SP in presence of PTX. This increase can be explained by the decrease of DSE. Since intracellular mechanisms of DSE and e-SP can occur within one presynaptic neuron, decrease of DSE causes increase of e-SP.

Differential intracellular signaling through specificity in G-proteins

Now it is known that effects might be depending on specific intracellular pathways, one might ask what determines which pathway is activated or not. At first, there are intercellular differences in intracellular background. Downstream intercellular enzymes may differ (Howlett, Blume & Dalton 2010). This is the case in for example the palette of adenylyl cyclase isoforms, which determines the outcome of cAMP response (Varga et al. 2008). The same might be said for G-protein availability, which can determine which pathway will be activated.
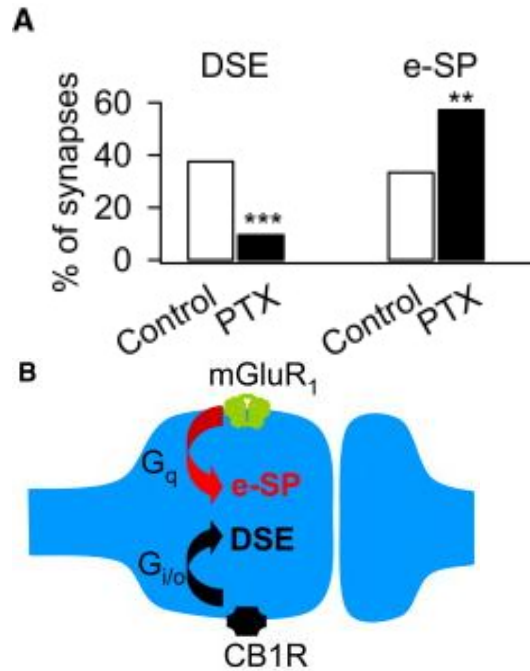
Figure 3.5: *The drop of DSE in presence of PTX shows that $G_{i/o}$ proteins mediate CB_1-induced DSE. In e-SP, the effect of endocannabinoids on astrocytes via CB_1 was shown to require PTX-insensitive CB_1-mediated signaling. Furthermore, the effect of glutamate released by astrocytes on presynaptic $mGluR_1$'s (shown in the left of B), is by coupling to a PTX-insensitive G protein (Navarrete, Araque 2010).*

A model for ligand specificity in activation of specific G-proteins

However, the most interesting form of specific activation is ligand specific activation. CB_1 ligands have big structural differences. Specific G-proteins meditate specific intracellular effects. Differential activation of the multiple G-proteins thereby leads to specific intracellular effects (Howlett, Blume & Dalton 2010). Different agonists can cause different ratios in signaling of specific G-proteins (Hudson, Hebert & Kelly 2010) (Varga et al. 2008). Based on response levels, a model of multiple possible mechanisms of changing conformation of GPCR has been proposed, which is shown in fig. 3.6. By a full agonist (A), the receptor favors G_i signaling over G_s. A partial agonist (B) causes a general decrease in strength of binding of G-proteins compared to a full agonist. Thereby, the G-proteins with relative high affinity, such as G_i, still bind to the receptor, while low affinity G-proteins, such as G_s, are not activated any longer.
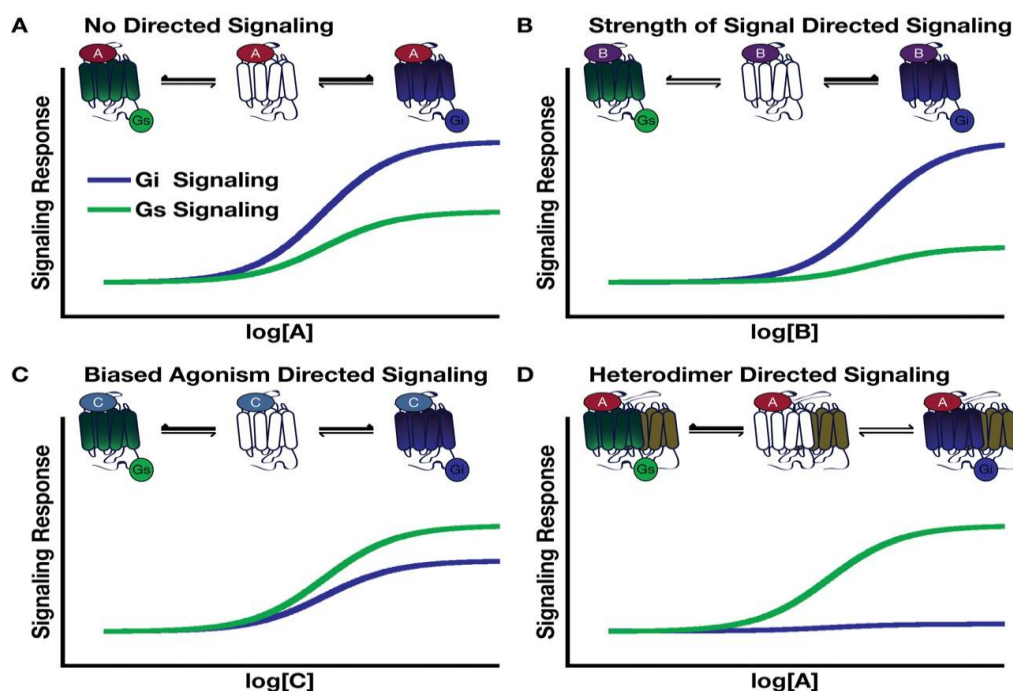
Figure 3.6: Model of GPCR conformations and the resulting concentration-response curves for ligand- and heterodimer- directed signaling. *This model includes the ligand specific signaling by strength of signaling effects (B) and biased agonism directed signaling (C) (Hudson, Hebert & Kelly 2010).*

The second form of ligand induced differences in signaling response is named true functional selectivity or biased agonism. In this case, the ligand stabilizes G_s binding conformation over that of G_i. Using plasmon-waveguide resonance (PWR) spectroscopy it was shown that differential G-protein activation is caused by differential changes in shape and or membrane orientation of CB_1, This leads to differences (Varga et al. 2008). Selectivity for a specific G-protein signaling is also possible through heterodimerization caused conformational changes of the receptor (Hudson, Hebert & Kelly 2010).

Ligand specificity in activation of specific G-proteins in practice

Differential activation by ligands has been shown at membranes of *Spodoptera frugiperda*, as shown in table 3.2. For example, HU 55,212-2 couples G_s comparable to $G_{i/o}$. However, WIN55,212-2 shows G-protein specificity.

Other research has shown that CP and anandamide have low affinity for G_s signaling. Because affinity of these two is also lower in $G_{i/o}$ signaling, their low effect on G_s is likely to be due to strength of signal effect (Hudson, Hebert & Kelly 2010).

	G_i activation		G_o activation	
	V_{max} (%)	EC_{50} (nM)	V_{max}	EC_{50}
HU-210	100	2.3 ± 0.3	100%	3.1 ± 0.3
WIN55,212-2	102 ± 4	330 ± 53	72 ±12	362 ± 93
Anandamide	92 ± 4	538 ± 54	71 ± 6	776 ± 78
THC	56 ± 6	196 ±13	64 ± 10	185 ± 28

Table 3.2: G-protein specificity of ligands at membranes of Spodoptera frugiperda. *The membranes were extracted using ultracentrifugation, after transfection of the suspended cells with human CB_1. Endogenous GTP-binding proteins were denatured by treatment with urea. Purified bovine brain G_i and G_o was added separately. Exchange from GDP to radioactive labeled, nonhydrolyzable [^{35}s]GTPγS was measured. Different agonists were found to activate these G-proteins differently (Glass, Northup 1999). See table 3.3. V_{max} is the maximal response by a given agonist, relatively compared to HU-210. EC_{50} represents the ligand concentration at which 50 percent of its maximal effect is achieved.*
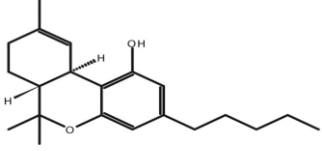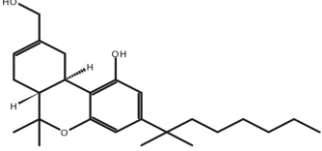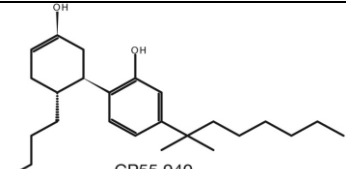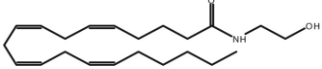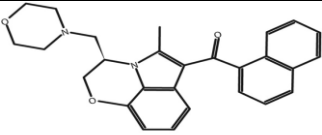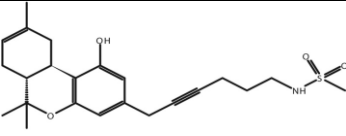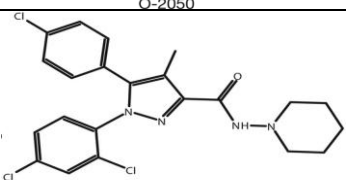
Ligand	Represents	G_i	G_0	G_s	$G_{q/11}$
THC	Classic cannabinoids	56%	?	?	N.E.
HU-210	Classic cannabinoids	100%	60-75%	Like $G_{i/o}$	N.E.
CP55,940	Non-classic cannabinoids	?	?	Low, poorly linked	N.E.
AEA Anandamide	Eicosonoids	100%	60-75%	Low	N.E.
WIN55212-2	Aminoalkylindoles	100%	60-75%	High	High
O-2050	Antagonist	?	?	?	?
SR141716	Inverse agonist	?	?	Blocks G_s, inverse agonist ?	?

Table 3.3: Functional selectivity of ligands for multiple G-proteins. At the left, this table shows the structure of multiple CB_1 ligands and the group of ligand-type they represent. Much more has to be determined yet. Since models are used, it should be noticed that they might not represent in vivo functioning. Comparing vertically, within a column, one individual G-protein can be differentially activated by ligands. Horizontally seen, within a row, one ligand might differentially activate the G-proteins. N.E. indicates no agonistic effect, probably neutral antagonistic effect. Question marks indicate lack of useful data (Glass, Northup 1999)(Abadji et al. 1999)(Hudson, Hebert & Kelly 2010).

CB_1 is a G-protein coupled receptor and thereby consists of seven trans-membrane parts, three extracellular and intracellular regions (Mukhopadhyay et al. 2002). Activation by classic cannabinoids was shown to depend on other receptor regions compared to non-classic cannabinoids (Mukhopadhyay et al.

2002). For example, mutating lysine 192 into alanine leads to a >100 reduction in effect size for classical cannabinoids while is does not affect WIN 55,212-2 efficiency (Varga et al. 2008).

It is suggested that CB_1 can adapt to multiple conformational states. This is suggested to cause changes in G-protein

activation sites, leading to different intracellular pathways (Varga et al. 2008).

The selectivity between G_s and G_i is shown to be mediated by the second intracellular loop of CB_1 (Varga et al. 2008). This was found in HEK293 cells, by cloning CB_1, inducing point mutations at different sited and measuring effect. Thereby, frame shifts were excluded. The residue Leu-222 is shown to be a critical determinant in G-protein coupling specificity.

Signal transduction pathways and functional ligand selectivity

Activation of CB_1 leads to activation of multiple cellular effects. These include $G_{i/o}$-mediated inhibition of VGCC, intracellular $[Ca^{2+}]$ effects and activation of inwardly rectifying K^+ channels, outward K^+ currents and voltage dependent Na^+ channels. Furthermore, effects on cAMP and MAPK are involved.

In addition, CB_1 is activated differentially by different ligands, having different activation of intracellular transduction pathways. Ligands are therefore suggested to have functional specificity.

Endogenous differences in activated pathways may also be due to intracellular differences rather than ligand specific activation. Table 3.3 summarizes the available *in vitro* results concerning relative differences in G-protein activation. Since cellular backgrounds is supposed to vary between cell types, translation to *in vivo* seems difficult. The results in this table do not concern these variations.

However, the results as demonstrated in the table can be interpreted in two ways. The first is that a single G-protein can be activated differently by different ligands. Furthermore, one ligand can be said to differentially activate G-proteins. These differences might also be the case in antagonizing CB_1. Therefore, the next chapter will focus on CB_1 antagonism and constitutive activity.

Inverse agonism and constitutive activity: a model

CB$_1$ is thought to have constitutive activity which can be blocked by an inverse agonist. A model of agonism, antagonism and inverse agonism is given in fig.4.1. The G-protein coupled receptor can be in either the inactive (R) state, or the active (R*) state (Aloyo et al. 2010). The active state * induces the stimulus, which causes the response. In the absence of ligands, the allosteric transition constant (L) represents the tendency of the receptor to be in the R* state rather than the R state. Presence of ligands (A) can alter the active/inactive-ratio of the receptor. When the ligand stabilizes R* more compared to R, it is an agonist. In this case $K_A/ K_A^* > 1$. A neutral antagonist blocks the agonist effect, but does not alter the active/inactive-ratio. Therefore, $K_A/ K_A^* = 1$. But in case of an inverse agonist, the inactive state of the receptor is promoted. Therefore, $K_A/ K_A^* < 1$ (Aloyo et al. 2010).
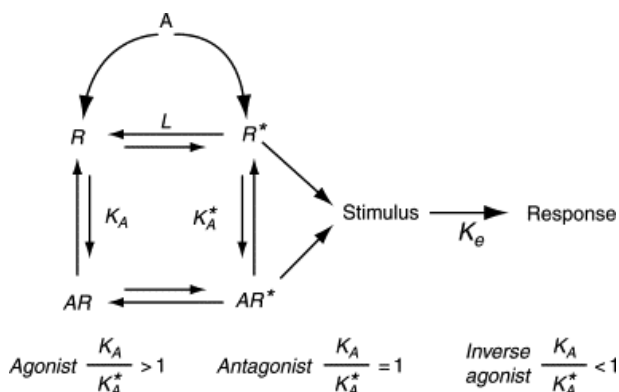

$Agonist \ \frac{K_A}{K_A^*} > 1 \quad Antagonist \ \frac{K_A}{K_A^*} = 1 \quad \substack{Inverse \\ agonist} \ \frac{K_A}{K_A^*} < 1$

Figure 4.1: Two-state model of GPCR activation. *In absence of ligand, the receptor, only L determines the ratio between activated receptor state (R*) compared to inactive state (R). Of ligand A, affinity constants can be determined for stabilizing the inactive (AR) and active receptor state (AR*). These are respectively $K_A = (R \times A)/AR$ and $K_A^* = (R^* \times A)/AR^*$. The ratio K_A/K_A^* determines what type of ligand it is (Aloyo et al. 2010).*

The stimulus size depends on the total density of receptors, R_T. Furthermore, response size depends on K_e, the efficiency with which an activated receptor induces the response. K_e can depend on availability of signal transduction molecules, for example G-proteins. R_T

and K_e together mediate the level of response and are cell and tissue specific.

The existence of a real neutral antagonist seems unlikely (Giraldo 2010). According to the described model, is should have exact the same affinity for the different R- and R*-state.

Ligand properties compose of receptor affinity and efficiency. In terms of efficiency, the multiple ligands should be seen in a continuum. The multiple ligands that have been found go from high efficiency agonists to neutral antagonist and inverse agonists gradually (Pertwee 2005). These properties represent differences in K_A/ K_A^*-ratios.

Ligand efficiency	K_A/K_A^*
High efficiency agonist	>>>1
Intermediate efficiency agonist	>>1
Low efficiency agonist	>1
Neutral antagonist	1
Inverse agonist	<1

The size of constitutive activity and inverse agonism

Size of constitutive activity sets the range in which inverse agonism can occur. The size of constitutive activity depends on three factors. At first, the allosteric transition constant (L) represents the size of constitutive activity. This can be compared with the receptors maximal effect reached in presence of agonists. The second factor is K_e, representing the efficiency with which a response is evoked. At third, receptor availability also determines the effect size of the maximal possible effect of an inverse agonist (Aloyo et al. 2010).

Practical work on inverse agonism and neutral antagonism by the author

Here, I would like to refer to the *appendix of this paper*, which concerns data of a patch clamping experiment on inverse agonism and neutral antagonism, which I have analyzed by myself. It includes electrophysiological measurements in the ventral tegmental area (VTA). The effects of both SR141716A and NESS on frequency and amplitude of EPSCs were tested by voltage clamp. Unfortunately, the results are not very clear and can therefore not be used in the argumentation of this paper.
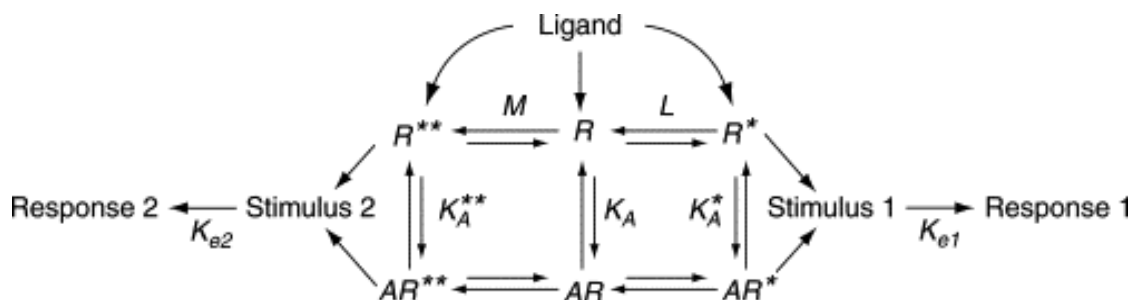
Figure 4.2: Three-state model of GPCR activation. *In addition to fig. 4.1, the ligand now consists of three association constants. [$K_A^{**} = (R^{**} \times A)/AR^{**}$], [$K_A^* = (R^* \times A)/AR^*$] and [$K_A = (R^* \times A)/AR$]. Multiple responses can be evoked, and a ligand might act differently on each receptor state (Aloyo et al. 2010).*

Inverse agonism in ligand specific response activation

In case of CB_1, a two state model of receptor activation might not sufficient, given its ligand specific activation. Therefore, a multiple-state model should be used. Now, as an example, a three-state model will be proposed (Aloyo et al. 2010). See Fig 4.2. Since CB_1 was shown to activate multiple G-protein in a ligand specific way, it must be concluded that CB_1 is able to have multiple active states, for example R^{**} and R^*, each with a specific response. In this case, two allosteric transition constants - M and L respectively - should be defined. Since pathway specific antagonism is mentioned (Giraldo 2010), stabilization or activation of a specific active state R^{**} or R^*, should be determined for each ligand independently. For example, an agonist specifically could induce response 1, $K_A/K_A^* > 1$, while K_A/K_A^{**} is unaffected. An inverse agonist specifically for response 2, should have a $K_A/K_A^{**} < 1$, while K_A/K_A^* is unaffected. However, it might also act as a neutral agonist for response 1, when in competition with agonists.

Agonists, inverse agonist and neutral antagonists combined.

In reality, different ligands will be available at the same time. This will lead to a complex situation, when having the described model in mind, which only describes the presence of one ligand. Furthermore, the effects of neutral antagonists and inverse agonists might be either competitive or non-competitive. For example, in case of a non-competitive neutral antagonist, there is competition within one and the same pathway (either the state R^* or R^{**}).

Inverse agonism and neutral antagonism in reality

Constitutive activity was shown to be increased in genetically modified mice, in which the C-terminal tail of the receptor (AA 418-472), was truncated (Abadji et al. 1999). The availability of this part in WT mice is thought to partially suppress constitutive activity. In terms of the model as described in fig. 4.1, R is normally transitioned into R^*, quantified by L. The transition into R^* is even more abundant in the mutant mouse.

Inverse agonism was not found only in unnatural systems with over expression of the receptor but has also been found in natural systems with realistic receptor concentrations (Pertwee 2005).

SR 141716A and AM 251 antagonize as an inverse agonist at high concentrations. However, at lower concentrations, is seems to act as a neutral antagonist. It is suggested that there are two sites of action.

At one site these substances displace agonists, at the other they induce inverse agonism, possible through an allosteric mechanism (Pertwee 2005) This can be described in terms of the model in fig 4.2. For example, R^* could be defined as the constitutive active state, due to a high constant L. At this site, the constitutive R^*-state can be diminished by high concentrations of SR 141716A. At this site $K_A/K_A^* < 1$.

At the other site, the R^{**}-state might be defined as the hardly constitutive activated state, due to a low constant M. Low concentrations antagonist interfere with agonist, but in absence of agonist, there is nothing left to block, while strictly seen, K_A/K_A^{**} still is < 1.

The second option for lack of inverse agonism at this site could be that constitutive active R** is present, but that SR141716 is neutral at this site, $K_A/K_A^* = 1$.

VCHSR, an analogue of SR141716A is said to be a neutral antagonist (Pertwee 2005). Both SR141716A and VCHSR showed antagonistic effects in presence of WIN55,212-2 by inhibition of Ca^{2+}-current inhibition in rat superior cervical ganglion neurons. However, in lack of WIN55,212-2, administration of VCHSR at 1 or 10 µM concentrations did not have an effect at all, in contract to SR 141716A.

O-2654 and O-2050, both analogues of Δ^8-THC, were also shown to act as neutral antagonists (Pertwee 2005). They are suggested to act as high-affinity, low-efficacy agonists. Inverse agonism might still be caused, since higher dosis have not been tested yet (Pertwee 2005).

NESS 0327, again an analogue of SR 141716, also behaved neutral in contrast to SR161714A (Ruiu et al. 2003). Furthermore it was shown to have a 10-fold higher effect if compared with SR141716A. NESS 0327 was the only CB_1 selective neutral antagonist yet tested in 2005, having a binding ratio CB_1/CB_2 of 60.000 (Pertwee 2006). Inverse agonism might still be caused, since higher doses have not been tested yet (Pertwee 2005).

Cellular effects: neutral vs. inverse agonism
It was hypothesized that neutral antagonist have effects different from those of an inverse agonist. Constitutive, basal CB_1 functioning it thought to cause other effects than specific functioning after activation of the receptor (Pertwee 2005).

Whether these two kinds of CB_1 functioning can be fully separated by pharmacological terms is doubted. Neutral antagonism suggests that the functioning of endocannabinoids is suppressed, while the basal, constitutive sort of functioning remains unaltered. In this definition however, possible tonic activity due to ongoing cannabinoid release should be defined as constitutive as well. The problem then is that the latter will also be

blocked by an antagonist that is neutral in terms of pharmacology (Pertwee 2005).

The desired therapeutic effects, such as reduction of food intake was thought to be due to neutral antagonism, while the adverse effects, such as nausea and depression are thought to be due to suppression of basal endocannabinoid functioning. If this is true, neutral antagonists would lead to drugs with less adverse effects (Pertwee 2005). This hypothesis seems to be a bit of wish full thinking, since it might have also been that adverse effects are due to neutral antagonism and the effects on food intake caused by inverse effects (Giraldo 2010).

However, behavioral experiments with antagonists that are thought to be neutral look promising (Bergman et al. 2008). For example, AM4113 does not induce taste aversion compared to SR 141716A, which was measured by vomiting and "con conditioned gaping" in rats (Bergman et al. 2008, Giraldo 2010). At the same time, in monkeys, food intake was still suppressed, with a < 3 fold decrease in potency, measured by lever presses (Bergman et al. 2008). More research with non-humans as well as humans is needed for a better understanding of the differences between natural antagonists and inverse agonist. Those experiments might yield a proper successor of Rimonabant.

CB_1 antagonism, an overview
Lately, research on CB_1 antagonism has focused on decreasing adverse effects by means of neutral antagonism. A model has been proposed, by which multiple findings can be explained. Cellular and electrophysiological effects have been found. (See the appendix for an example of an experimental setup of these kinds of experiments!).

Furthermore, behavioral differences were found between neutral and inverse agonists. These results look promising for therapeutic purpose. However, at the same time complete loss of behavioral and psychiatric adverse effects by only the single concept of neutral antagonism may seem wishful thinking. Ligand specific antagonism is theoretically supposed, and research should reveal its relevance.

Discussion

For antagonizing CB_1, many aspects should be taken into account. These include endogenous cellular differences in functioning between brain regions, but also tissues and cell types. Furthermore, the quality and quantity of (non-endogenous) ligand specific effects should be studied. Namely, a ligand's potency for effecting specific receptor states could change region-, tissue-, and cell type-specific effects differentially. This difference might be the next step in the extraction of adverse effects from the beloved therapeutic possibilities of CB_1 antagonists.

Furthermore, the role of astrocytes can also been shown in a complete other perspective. Since the potentiating role of endocannabinoids is shown, it can be deduced anyhow that the interfering CB_1 with antagonists or inverse agonists, not only cause relative increase of excitatory neurotransmitter release, but also a relative decrease of excitatory neurotransmitter release, compared to proper endocannabinoid functioning.

Wishful thinking it seems to expect a complete distinction of adverse and therapeutic effects, based on a single pharmacological difference. It might therefore be better to speak of an improved balance between adverse and therapeutic effects, such as is definitely the case in distinguishing neutral and inverse agonism. Cell type specific antagonism might also improve the balance between adverse and therapeutic effects.

Many of the experiments that have been performed regarding functional selectivity depend on agonists in cell cultures, often with an unnatural high expression of CB_1. Since region-, tissue-, and cell type-specific effects by the different ligands were never been tested, the size and importance is yet to be determined. The parameters involved in this specificity will now be discussed.

The total receptor density (R_T) is specific for cell type and tissue. However, it seems unlikely that ligands can differentially affect cell types or tissues by this parameter, since specificity is not involved. On the other hand, the absolute effect of antagonizing CB_1 is higher in a cell with high receptor density relative to cells with low receptor density.

K_E indicates the effect size of an activated receptor state, depending on for example specific G-protein availability and downstream transduction pathways. The absolute effect of antagonizing CB_1 is higher in a cell with relative high K_E.

In contrast to R_T and K_E, real *relative* differences between region, tissue, and cell type, can be mediated by the antagonist's differences in K_A/K_A*-ratio for multiple states. Namely, cells differ in potentiating a response after activation of a specific receptor state. Therefore, the specific antagonist could cause both quantitative and qualitative effects, relative to its status quo but also relative to antagonized situation at cells from other regions, tissues, and cell types. This antagonism could be compared with biased agonism as described in the second chapter, rather than strength of signal differences. These findings however suggest that the distinction of receptor states is probably more a different ratio between the states rather than dichotomy, in which specific pathways are completely activated or not activated at all.

A speculated example will now follow, describing the possible distinction of CB_1 functioning in astrocytes and neurons by an antagonist. Astrocytes potentiating neurotransmission has so far only been shown in hippocampal CA-3 CA-1 synapses, but might be present in other brain regions as well. Namely, the paradigm shift from neuronal to neuron-glia networks is recent (Araque, Navarrete 2010) and involvement of glia cells is therefore explored much less thoroughly as neuronal pathways. At this moment, this might lead to a biased view and an underestimation of glial functioning. Since cannabinoids' effect on neurons is proven to mainly depend on activation of $G_{i/o}$ but the effect via astrocytes on non-$G_{i/o}$-G-proteins, antagonists might differentially act on these cell types. This ligand could be identified by electrophysiological experiments and could be used to distinguish the behavioral effects of CB_1 antagonism underlying neurons or astrocytes.

	Cell type: Neuron	**Cell type B: Astrocyte**
Endogenous (non-specific agonist)	State I $\rightarrow$ **$G_{I/O}$** $\rightarrow$ **response I** State II$\rightarrow$ G_S	State I $\rightarrow$ $G_{I/O}$ State II$\rightarrow$ **G_S** $\rightarrow$ **response II**
+ Antagonist State I	State I $\rightarrow$ **$G_{I/O}$** $\rightarrow$ ~~response I~~ State II$\rightarrow$ G_S	State I $\rightarrow$ $G_{I/O}$ State II$\rightarrow$ **G_S** $\rightarrow$ **response II**
+ Antagonist State II	State I $\rightarrow$ **$G_{I/O}$** $\rightarrow$ **response I** State II$\rightarrow$ G_S	State I $\rightarrow$ $G_{I/O}$ State II$\rightarrow$ **G_S** $\rightarrow$ ~~response II~~

Figure 5.1: Cell type specific CB_1 antagonism. *Cell type A depends on activation of $G_{I/o}$ by receptor state I. Cell type B depends on activation of G_S by receptor state II. Antagonism specific for receptor state I causes inactivation of the response in cell type A, but not cell type B. Vice versa, cell type B will be specifically blocked by an antagonist specific for receptor state II. Red stands for antagonized, green for unaffected.*

I define activation of the $G_{i/o}$-protein to be mediated by Receptor State I and the activation astrocytes by the non-$G_{i/o}$-protein dependent pathway mediated by Receptor State II (probably G_S). This is shown in fig. 5.1. When the ligand would be more potent in antagonizing state I rather than state II, the CB_1 functioning is more absent in neurons compared to astrocytes. A state II specific antagonist would block astrocytes, but leave the neuronal functioning more intact.

Such a difference might already be the case in antagonizing CB_1, for example in treatment with SR141716A. This seems unlikely for AM251, since it was shown to block both DSE and e-SP. Therefore, antagonists could be specially formed or selected based on these properties.

Experiments with mutations at specific regions of CB_1 have already revealed much about the responsible receptor parts. This might be useful for selecting candidate molecules.

Further experiments

A realistic approach for selecting candidate molecules would be high throughput screening in which the relative difference between on Ca^{2+} elevation in cultured astrocytes and $G_{I/O}$ activation in cultured neurons is determined. Great relative differences might prospect cell type specificity.

The actual effect of cell type specific antagonism should be quantified using electrophysiology after neural depolarization such as (Navarrete, Araque 2010). The percentage of heteroneuronal synapses expressing e-SP rather than DSE could be determined in the hippocampal CA3 – CA1 neurons.

The mean amplitude of responses in pA, including failures of neurotransmission, should be compared, which is known as synaptic efficiency. Second, probability of neurotransmitter release should be determined. Furthermore, the mean EPSC amplitude excluding failures could be measured and compared for different antagonists.

Whether this is realistic is to be determined. This would also reveal to what extent the differences between astrocyte and neurons are due to activation of different receptor states or due to differences in intracellular pathways such as G-protein palette of downstream targets.

Furthermore it is interesting to determine differences in constitutive activity between neurons and glia cells. Constitutive activity in the form of tonic release of endocannabinoids seems however unlikely to be different between neurons and astrocytes. Namely, it is the endocannabinoid that is released tonic and therefore able to activate both

neuronal and glial cells with the same intensity.

In contrast, higher constitutive activity by the receptor itself could be possible. For example, if constitutive activity in neurons is much greater than in astrocytes, than the effect of an inverse agonist will have a much greater impact for neurons than for astrocytes and therefore change the balance. Constitutive activity however seems hard to detect with electrophysiology and even harder it is to notice differences in it.

Conclusion

The described type of research could be of high value for understanding CB_1 antagonism and cell type specificity. However, the significance and size of the proposed mechanism of antagonism on a cellular level should be determined. Even more uncertain are the implications for effects on a behavioral level. Therefore, testing a proposed compound on a behavioral level will be the only ultimate test.

However, proving and understanding the mechanism of cell type specific CB_1 antagonism at a molecular and cellular level, could be of important value for the invention and fine-tuning of a useful and welcome drug.

References

Abadji, V., Lucas-Lenard, J.M., Chin, C. & Kendall, D.A. 1999, "Involvement of the carboxyl terminus of the third intracellular loop of the cannabinoid CB1 receptor in constitutive activation of Gs", *Journal of neurochemistry,* vol. 72, no. 5, pp. 2032-2038.

Aloyo, V.J., Berg, K.A., Clarke, W.P., Spampinato, U. & Harvey, J.A. 2010, "Inverse agonism at serotonin and cannabinoid receptors", *Progress in molecular biology and translational science,* vol. 91, pp. 1-40.

Araque, A. & Navarrete, M. 2010, "Glial cells in neuronal network function", *Philosophical transactions of the Royal Society of London.Series B, Biological sciences,* vol. 365, no. 1551, pp. 2375-2381.

Bergman, J., Delatte, M.S., Paronis, C.A., Vemuri, K., Thakur, G.A. & Makriyannis, A. 2008, "Some effects of CB1 antagonists with inverse agonist and neutral biochemical properties", *Physiology & Behavior,* vol. 93, no. 4-5, pp. 666-670.

Bisogno, T., Howell, F., Williams, G., Minassi, A., Cascio, M.G., Ligresti, A., Matias, I., Schiano-Moriello, A., Paul, P., Williams, E.J., Gangadharan, U., Hobbs, C., Di Marzo, V. & Doherty, P. 2003, "Cloning of the first sn1-DAG lipases points to the spatial and temporal regulation of endocannabinoid signaling in the brain", *The Journal of cell biology,* vol. 163, no. 3, pp. 463-468.

Christensen, R., Kristensen, P.K., Bartels, E.M., Bliddal, H. & Astrup, A. 2007, "Efficacy and safety of the weight-loss drug rimonabant: a meta-analysis of randomised trials", *Lancet,* vol. 370, no. 9600, pp. 1706-1713.

De Petrocellis, L. & Di Marzo, V. 2009, "An introduction to the endocannabinoid system: from the early to the latest concepts", *Best practice & research.Clinical endocrinology & metabolism,* vol. 23, no. 1, pp. 1-15.

Demuth, D.G. & Molleman, A. 2006a, "Cannabinoid signalling", *Life Sciences,* vol. 78, no. 6, pp. 549-563.

Demuth, D.G. & Molleman, A. 2006b, "Cannabinoid signalling", *Life Sciences,* vol. 78, no. 6, pp. 549-563.

Devane, W.A., Dysarz, F.A.,3rd, Johnson, M.R., Melvin, L.S. & Howlett, A.C. 1988, "Determination and characterization of a cannabinoid receptor in rat brain", *Molecular pharmacology,* vol. 34, no. 5, pp. 605-613.

Devane, W.A., Hanus, L., Breuer, A., Pertwee, R.G., Stevenson, L.A., Griffin, G., Gibson, D., Mandelbaum, A., Etinger, A. & Mechoulam, R. 1992, "Isolation and structure of a brain constituent that binds to the cannabinoid receptor", *Science (New York, N.Y.),* vol. 258, no. 5090, pp. 1946-1949.

Di Marzo, V. 2011, "Endocannabinoid signaling in the brain: biosynthetic mechanisms in the limelight", *Nature neuroscience,* vol. 14, no. 1, pp. 9-15.

Di Marzo, V. 2009, "The endocannabinoid system: its general strategy of action, tools for its pharmacological manipulation and potential therapeutic

exploitation", *Pharmacological research : the official journal of the Italian Pharmacological Society,* vol. 60, no. 2, pp. 77-84.

Di Marzo, V. 2008, "Targeting the endocannabinoid system: to enhance or reduce?", *Nature reviews.Drug discovery,* vol. 7, no. 5, pp. 438-455.

Di Marzo, V., De Petrocellis, L., Sugiura, T. & Waku, K. 1996, "Potential biosynthetic connections between the two cannabimimetic eicosanoids, anandamide and 2-arachidonoyl-glycerol, in mouse neuroblastoma cells", *Biochemical and biophysical research communications,* vol. 227, no. 1, pp. 281-288.

Di Marzo, V., Fontana, A., Cadas, H., Schinelli, S., Cimino, G., Schwartz, J.C. & Piomelli, D. 1994, "Formation and inactivation of endogenous cannabinoid anandamide in central neurons", *Nature,* vol. 372, no. 6507, pp. 686-691.

Di Marzo, V., Goparaju, S.K., Wang, L., Liu, J., Batkai, S., Jarai, Z., Fezza, F., Miura, G.I., Palmiter, R.D., Sugiura, T. & Kunos, G. 2001, "Leptin-regulated endocannabinoids are involved in maintaining food intake", *Nature,* vol. 410, no. 6830, pp. 822-825.

Edwards, D.A., Kim, J. & Alger, B.E. 2006, "Multiple mechanisms of endocannabinoid response initiation in hippocampus", *Journal of neurophysiology,* vol. 95, no. 1, pp. 67-75.

Gaoni, Y. & Mechoulam, R. 1964, "Isolation, structure and partial synthesis of an active constituent of hashish", *Journal of the American Chemical Society,* .

Gerdeman, G.L., Ronesi, J. & Lovinger, D.M. 2002, "Postsynaptic endocannabinoid release is critical to long-term depression in the striatum", *Nature neuroscience,* vol. 5, no. 5, pp. 446-451.

Giraldo, J. 2010, "How inverse can a neutral antagonist be? Strategic questions after the rimonabant issue", *Drug discovery today,* vol. 15, no. 11-12, pp. 411-415.

Glass, M. & Northup, J.K. 1999, "Agonist selective regulation of G proteins by cannabinoid CB(1) and CB(2) receptors", *Molecular pharmacology,* vol. 56, no. 6, pp. 1362-1369.

Grunfeld, Y. & Edery, H. 1969, "Psychopharmacological activity of the active constituents of hashish and some related cannabinoids", *Psychopharmacologia,* vol. 14, no. 3, pp. 200-210.

Herkenham, M. *Distribution of brain CB_1 receptors*.

Howlett, A.C., Blume, L.C. & Dalton, G.D. 2010, "CB(1) cannabinoid receptors and their associated proteins", *Current medicinal chemistry,* vol. 17, no. 14, pp. 1382-1393.

Hudson, B.D., Hebert, T.E. & Kelly, M.E. 2010, "Ligand- and heterodimer-directed signaling of the CB(1) cannabinoid receptor", *Molecular pharmacology,* vol. 77, no. 1, pp. 1-9.

Kano, M., Ohno-Shosaku, T., Hashimotodani, Y., Uchigashima, M. & Watanabe, M. 2009, "Endocannabinoid-mediated control of synaptic transmission", *Physiological Reviews,* vol. 89, no. 1, pp. 309-380.

Kirkham, T.C. 2005, "Endocannabinoids in the regulation of appetite and body weight", *Behavioural pharmacology,* vol. 16, no. 5-6, pp. 297-313.

Kreitzer, A.C. & Regehr, W.G. 2001, "Retrograde Inhibition of Presynaptic Calcium Influx by Endogenous Cannabinoids at Excitatory Synapses onto Purkinje Cells", *Neuron,* vol. 29, no. 3, pp. 717-727.

Kushmerick, C., Price, G.D., Taschenberger, H., Puente, N., Renden, R., Wadiche, J.I., Duvoisin, R.M., Grandes, P. & von Gersdorff, H. 2004, "Retroinhibition of presynaptic Ca2+ currents by endocannabinoids released via postsynaptic mGluR activation at a calyx synapse", *The Journal of neuroscience : the official journal of the Society for Neuroscience,* vol. 24, no. 26, pp. 5955-5965.

Kwatra, S.G. 2010, "Termination of the CRESCENDO trial", *Lancet,* vol. 376, no. 9757, pp. 1984; author reply 1984-5.

Le Foll, B., Gorelick, D.A. & Goldberg, S.R. 2009, "The future of endocannabinoid-oriented clinical research after CB1 antagonists", *Psychopharmacology,* vol. 205, no. 1, pp. 171-174.

Lovinger, D.M. 2008, "Presynaptic modulation by endocannabinoids", *Handbook of Experimental Pharmacology,* vol. (184), no. 184, pp. 435-477.

Maejima, T., Hashimoto, K., Yoshida, T., Aiba, A. & Kano, M. 2001, "Presynaptic Inhibition Caused by Retrograde Signal from Metabotropic Glutamate to Cannabinoid Receptors", *Neuron,* vol. 31, no. 3, pp. 463-475.

Matsuda, L.A., Lolait, S.J., Brownstein, M.J., Young, A.C. & Bonner, T.I. 1990, "Structure of a cannabinoid receptor and functional expression of the cloned cDNA", *Nature,* vol. 346, no. 6284, pp. 561-564.

Mattes, R.D., Engelman, K., Shaw, L.M. & Elsohly, M.A. 1994, "Cannabinoids and appetite stimulation", *Pharmacology, biochemistry, and behavior,* vol. 49, no. 1, pp. 187-195.

Mechoulam, R. & Shvo, Y. 1963, "The structure of cannabidiol", *Tetrahedron,* .

Mechoulam, R., Feigenbaum, J.J., Lander, N., Segal, M., Jarbe, T.U., Hiltunen, A.J. & Consroe, P. 1988, "Enantiomeric cannabinoids: stereospecificity of psychotropic activity", *Experientia,* vol. 44, no. 9, pp. 762-764.

Mechoulam, R., Lander, N., Varkony, T.H., Kimmel, I., Becker, O., Ben-Zvi, Z., Edery, H. & Porath, G. 1980, "Stereochemical requirements for cannabinoid activity", *Journal of medicinal chemistry,* vol. 23, no. 10, pp. 1068-1072.

Mitterdorfer, J. & Bean, B.P. 2002, "Potassium currents during the action potential of hippocampal CA3 neurons", *The Journal of neuroscience : the official journal of the Society for Neuroscience,* vol. 22, no. 23, pp. 10106-10115.

Mukhopadhyay, S., Shim, J., Assi, A., Norford, D. & Howlett, A.C. 2002, "CB1 cannabinoid receptor-G protein association: a possible mechanism for differential signaling", *Chemistry and physics of lipids,* vol. 121, no. 1-2, pp. 91-109.

Munro, S., Thomas, K.L. & Abu-Shaar, M. 1993, "Molecular characterization of a peripheral receptor for cannabinoids", *Nature,* vol. 365, no. 6441, pp. 61-65.

Navarrete, M. & Araque, A. 2010, "Endocannabinoids potentiate synaptic transmission through stimulation of astrocytes", *Neuron,* vol. 68, no. 1, pp. 113-126.

Navarrete, M. & Araque, A. 2008, "Endocannabinoids mediate neuron-astrocyte communication", *Neuron,* vol. 57, no. 6, pp. 883-893.

Nicholson, R.A., Liao, C., Zheng, J., David, L.S., Coyne, L., Errington, A.C., Singh, G. & Lees, G. 2003, "Sodium channel inhibition by anandamide and synthetic cannabimimetics in brain", *Brain research,* vol. 978, no. 1-2, pp. 194-204.

Ohno-Shosaku, T., Maejima, T. & Kano, M. 2001, "Endogenous Cannabinoids Mediate Retrograde Signals from Depolarized Postsynaptic Neurons to Presynaptic Terminals", *Neuron,* vol. 29, no. 3, pp. 729-738.

Pertwee, R.G. 2006, "The pharmacology of cannabinoid receptors and their ligands: an overview", *International journal of obesity (2005),* vol. 30 Suppl 1, pp. S13-8.

Pertwee, R.G. 2005, "Inverse agonism and neutral antagonism at cannabinoid CB1 receptors", *Life Sciences,* vol. 76, no. 12, pp. 1307-1324.

Rinaldi-Carmona, M., Barth, F., Heaulme, M., Shire, D., Calandra, B., Congy, C., Martinez, S., Maruani, J., Neliat, G. & Caput, D. 1994, "SR141716A, a potent and selective antagonist of the brain cannabinoid receptor", *FEBS letters,* vol. 350, no. 2-3, pp. 240-244.

Ruiu, S., Pinna, G.A., Marchese, G., Mussinu, J.M., Saba, P., Tambaro, S., Casti, P., Vargiu, R. & Pani, L. 2003, "Synthesis and characterization of NESS 0327: a novel putative antagonist of the CB1 cannabinoid receptor", *The Journal of pharmacology and experimental therapeutics,* vol. 306, no. 1, pp. 363-370.

Starowicz, K., Nigam, S. & Di Marzo, V. 2007, "Biochemistry and pharmacology of endovanilloids", *Pharmacology & therapeutics,* vol. 114, no. 1, pp. 13-33.

Varga, E.V., Georgieva, T., Tumati, S., Alves, I., Salamon, Z., Tollin, G., Yamamura, H.I. & Roeske, W.R. 2008, "Functional selectivity in cannabinoid signaling", *Current molecular pharmacology,* vol. 1, no. 3, pp. 273-284.

Varma, N., Carlson, G.C., Ledent, C. & Alger, B.E. 2001, "Metabotropic glutamate receptors drive the endocannabinoid system in hippocampus", *The Journal of neuroscience : the official journal of the Society for Neuroscience,* vol. 21, no. 24, pp. RC188.

Wilson, R.I. & Nicoll, R.A. 2001, "Endogenous cannabinoids mediate retrograde signalling at hippocampal synapses", *Nature,* vol. 410, no. 6828, pp. 588-592.

Xiong, W., Cheng, K., Cui, T., Godlewski, G., Rice, K.C., Xu, Y. & Zhang, L. 2011, "Cannabinoid potentiation of glycine receptors contributes to cannabis-induced analgesia", *Nature chemical biology,* .

Appendix: Patch clamp recordings of CB_1 inverse agonism and neutral antagonism in the mouse Ventral Tegmental Area (VTA).

Remco Molenhuis

Research Project Mini-Internship
Bachelor Biomedical Sciences
Utrecht University

R.T.Molenuis@students.uu.nl
Student number: 3384470

Supervisors: Dr. Geert Ramakers, Frank Meye and Granville Matheson

Overview

This appendix is about the practical side of patch clamping experiments in the Ventral Tegmental Area (VTA) on mouse brain slices. Practical lab work was done during a one-week internship, including pretreating C57BL/6J mice with certain compounds, sacrificing them, isolating and slicing their brains, keeping the cells alive controlling the right circumstances and electrophysiological recordings in multiple conditions. Steps 1, 2 and 3 describe this practical work. Next, data of VTA patch clamping experiments was processed in Excel, which is described in steps 4 and 5. The experiments, whose data was used for processing, were performed in the presence of compounds either considered to be neutral antagonist (NESS0327) or inverse agonist (SR141716A). Unfortunately, this data was not gathered during the internship, since experiments that were performed during the internship didn't focus on inverse agonism and neutral antagonism. As suggested in the main part of this thesis, NESS0327 was expected to have greater effects on EPSC frequency compared to SR141716A. For processing the data, many statistical and computational aspects were taken into account. Sadly, differences between EPSC's (frequency and amplitude) in presence of either neutral antagonist (NESS0327) or inverse agonist (SR141716A) were not very satisfying.

Step1: From mice to slice

To obtain slices of the VTA, the C57BL/6J mice were sacrificed. The mice should be of relative young age, since patch clamping in older mice is harder because of fibers. The mouse was put into a box with vaporized iso-flurane. After a few seconds, the mouse was decapitated and its brain isolated. To yield healthy cells, this was performed fast and it was put into the ice-cold medium as soon as possible. This medium included stock ACSF (artificial cerebrospinal fluid), which was made out of two pre-stocks which needed to be diluted ten times. Stock ACSF was also perfused with 95% O_2 and 5% CO_2 (acid buffer). The ice-cold medium furthermore included ascorbic acid and Mg^{2+} ($MgSO_4$) to prevent cell damage due to neuronal over-firing caused by isolation and slicing.

ACSF:	Final concentration:
Stock 1	
NaCl	124 mM
KCl	3.3 mM
KH_2PO_4	1.2 mM
$MgSO_4 * 7 H_2o$	1.3 mM
$CaCl_2 * 2 H_2o$	2.5 mM
Stock 2	
$NaHCO_3$	20 mM
Glucose	10 mM

Of the brain, the frontals and cerebellum were cut off. Then the brain was rolled onto the frontal. Then the dorsal side of the brain was cut off. This surface of the brain was glued onto a plate, which was put into the Vibratome. 200 micrometer thick slices were made for patch clamping, see figure 1.1. In contrast, 350 micrometers is the thickness used for measuring field potentials (e.g. fEPSP's or fIPSP's). The slices were cut into halves and kept in a warm ACSF bath, perfused with 95% O_2 and 5% CO_2 (acid buffer).
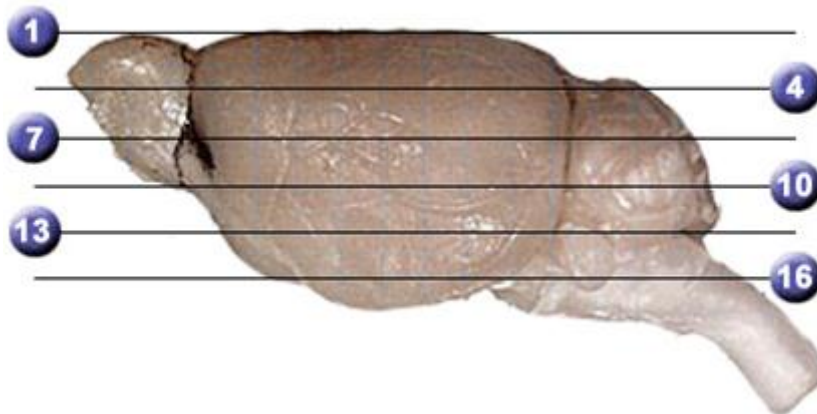
Figure 1.1: cutting brain slices. *This figure shows the slicing direction of the Vibratome. After cutting of the frontals (left) and cerebellum (right), the dorsal side was cut off. The brain was glued onto the Vibratome with the dorsal side (upside down compared to the image). Indeed, slices of 200 micrometers were made, starting ventral (16 in this figure) ending dorsal (1 in this figure).The VTA should be found around level 13.* (http://www.mbl.org/atlas232/atlas232_frame.html)

Step 2: Identifying recordable cells in the VTA

A slice, from around level 13 as indicated in figure 1.1, was put under the microscope. In practice, VTA containing slices were predicted as follows. Cutting slice after slice, starting ventral, the presence of the cerebellar connection is a good predictor. These slices were used. Under the microscope, the VTA was found next and between the MT (see figure 2) and fiber tracts of the lemniscus (ml) (see figure 2.1 and 2.2). Presynapses that are found in the VTA are generally afferents from lower regions. Postsynapses that are found in the VTA generally are from cells of the VTA. Therefore, recording of VTA neurons is recording this single type of synapses.
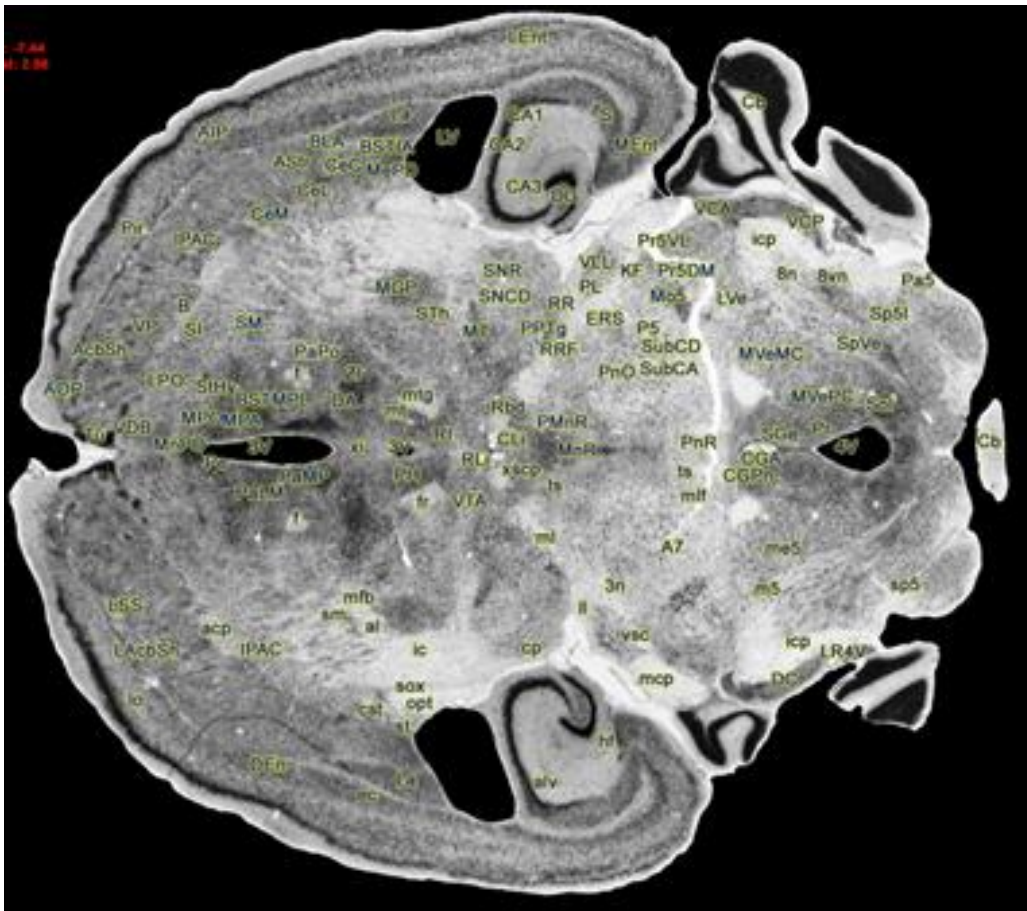
Figure 2.1: C57BL/6J mouse brain anatomy: VTA: level 12. This microscopic section (horizontal) was made at level 12 as indicated in figure 1.1. In the middle, VTA and ml (lemniscus) are indicated. (http://www.mbl.org/atlas232/atlas232_frame.html)
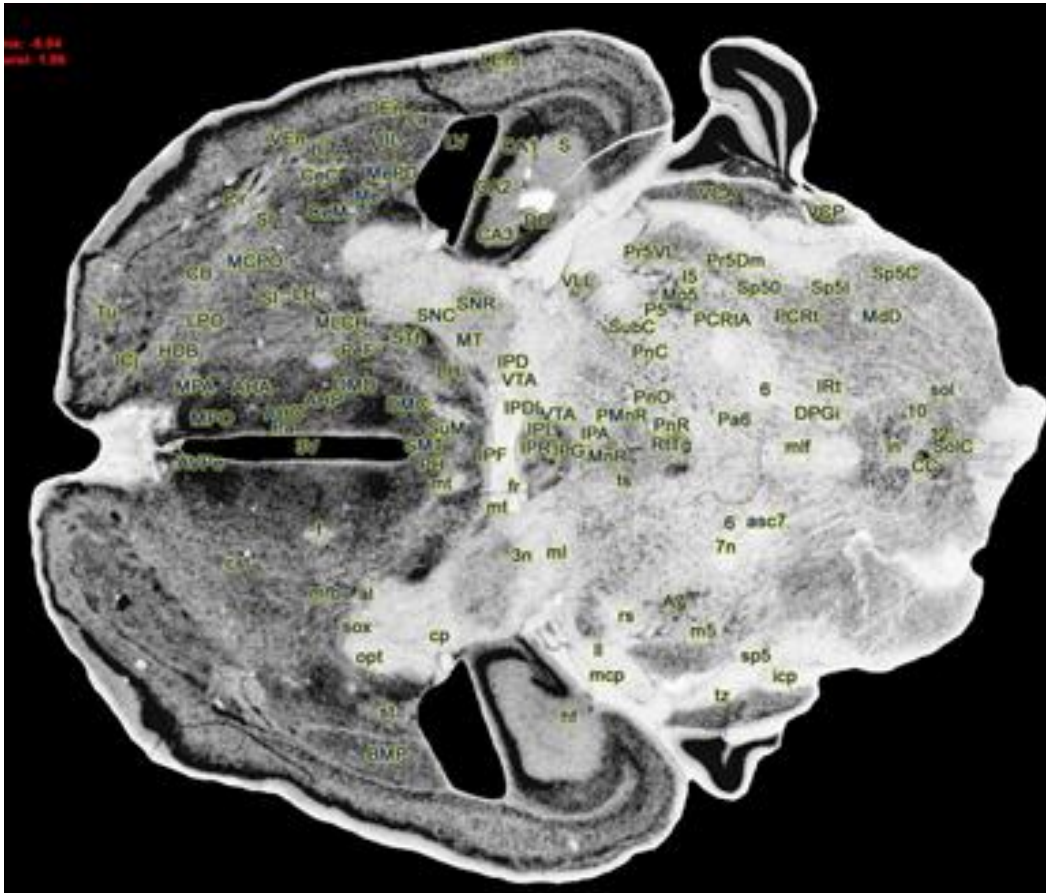
Figure 2.2: C57BL/6J mouse brain anatomy: VTA: level 13. *This microscopic section (horizontal)was made at level 13 as indicated in figure 1.1. In the middle, VTA, MT and ml (lemniscus) are indicated.* (http://www.mbl.org/atlas232/atlas232_frame.html)

Specific for this experiment, about the influence of morphine on CB_1 electrophysiology in the VTA, recorded cells needed to be dopaminergic. Dopaminergic neurons were identified by fluorescence. In these mice, PitX3, a transcription factor which is specific for dopaminergic neurons, contained GFP. By this means, dopaminergic neurons in the VTA were selected.

In absence of PitX3-GFP mice, this was done by checking the existence of H-currents, showing presence of inwardly rectifying K^+ channels, which is also specific for dopaminergic neurons in the VTA. This was however done in current-clamp conditions rather than voltage clamp. Negative current pulses were increased step-wise (steps of 10 mV). An increase of the voltage needed to maintain the set current during a pulse, indicates inwardly rectifying K^+ channels. Indeed, these cells compensate for polarization. A difference between the current which is needed at the beginning and at the end of a pulse, indicates compensation. Furthermore, Cesium could not be used in the internal medium (see step 3).

Step 3: Whole cell current clamp recordings

During the experiment, the external environment was perfused ASCF, containing gas of 95% O_2 and 5% CO_2 (acid buffer). TTX was added to block action potentials by voltage-gated Na^+-channels. In this experiment, miniEPSCs (mEPSC's) were determined. In contrast, TTX should absolutely not be used or sporadic present when measuring field potentials.

Furthermore there is an artificial internal medium, which is inside the pipette. The internal medium contained TEA and Cesium to block potassium channels. Indeed, this experiment focused on mEPSP's. GABA-eric receptors are situated on the dendrite more closely to the soma compared to glutamate receptors. This leads GABA to have a higher amplitude and decay of a signal.

Pipettes were made using the pipette-puller. The set-up of this apparatus is important since it determines diameter and resistance of the pipette. Installed on the recording set-up, with the internal medium inside the pipette, the resistance was measured. A reference electrode was used. Resistance of about 5 MΩ indicates a clean pipette, having no dust stuck inside.

Cells were selected based on morphology, suing microscopy. Absence of nucleus and proper membrane indicate good recordable cells. The cell was approached by the pipette and a giga-seal was made. This was done by adding negative pressure to the pipette by sucking it. Seal was indicated by a change in resistance from about 5 MΩ to 1 GΩ.

To compensate for fast capacity transients, mainly caused by the pipette capacitance to bath, **C-fast** was set. This is shown in figure 3.1
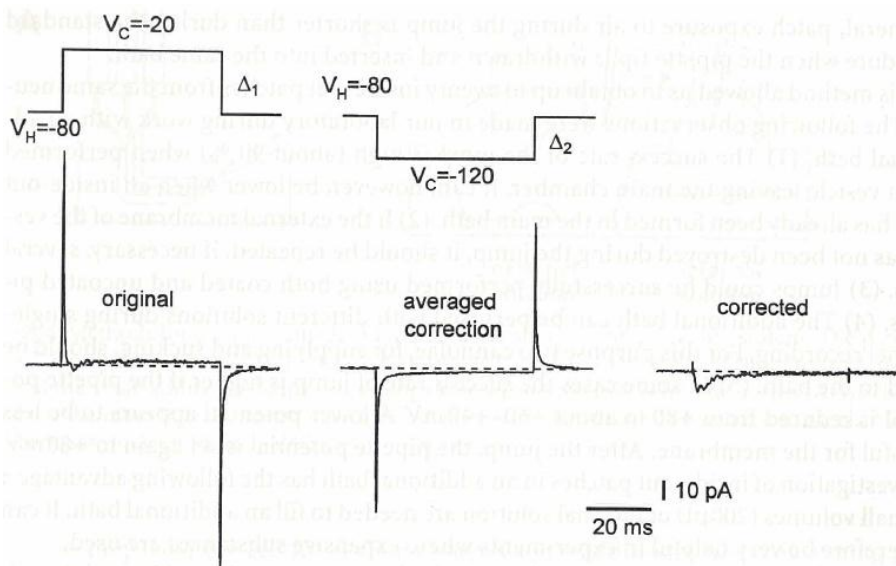

Figure 3.1: Compensating C-fast. *Leakage current and transient capacity currents are subtracted from the recording. The left shows an original recording, the middle the subtraction and on the right the final recorded Na^+ current is shown, after processing. (Uwe Windhorst, Håkan Johansson, Modern techniques in neuroscience research, Springer, 1999)*

Following the giga-seal, whole cell recording was made by applying strong suction. 300 MΩ was used to indicate a good connection. Holding potential (V_h) was set to -60 mV. A 5mV (command potential V_c), 5ms pulse was added. **C-slow**, compensating for the cell's membrane capacitance, was set. An example is a C-slow of 26.19 pF. The range was set to 100 pF.

R-series, the resistance of the electrical circuit, was calculated and compensated. See figure 3.2. Because the voltage was set at 5mV, and the current was found during using the earlier described pulse, resistance was calculated using the formula R=U/I. (For example, U_{set}=5mV, I_{needed}=260pA → R-series was found and said to be 13.7 MΩ.
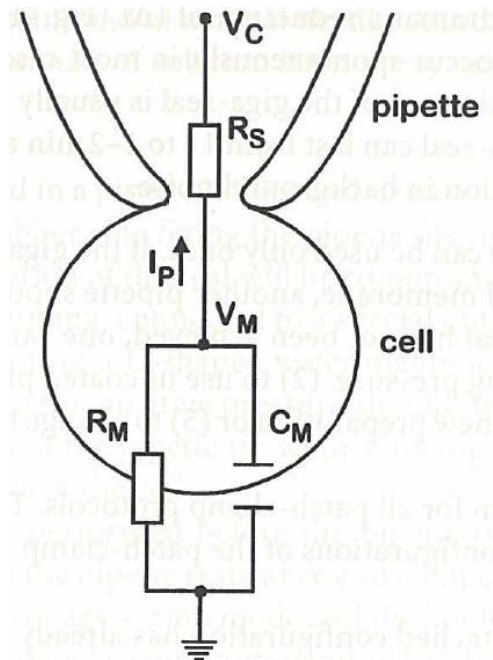

Figure 3.2: The existence of and compensation for series resistance. *Because of the series resistance (R_s), the membrane potential (V_m) is not the same as the command voltage (V_c). After calculating R_s as indicated in the text, R_s can and must be compensated. (Uwe Windhorst, Håkan Johansson, Modern techniques in neuroscience research, Springer, 1999)*

Next, the neuron was checked and baseline activity was measured. After having this done for about 20 minutes, compound was added. Unfortunately, the compounds that were used during these experiments differ from those of the data that will be discussed in the next chapter. However, the concept and experimental set-up are very much the same.

Step 4: Processing data: individual experiments

As mentioned in the overview of this appendix, the data that have been used for processing are not those gathered during the mini-internship. During voltage clamp experiments, NESS0327 or SR141716A was added (or both). The desired output is a graph showing time-frequency and time-amplitude. Since the number of events is huge, averages are determined over epochs of 2 minutes. Differences between NESS0327 and SR141716A are expected. Since endocannabinoids act presynaptic, one might expect a frequency effect rather than an amplitude effect.

During the experiment, the criteria for an **event** are set by multiple parameters (preferably with high specificity and selectivity). These include relative differences in amplitude compared to a previous time interval. The result is a data set with *events* (reflecting mEPSC's) that match these criteria. Of each event, time (ms) and amplitude (pA) are in this data set among others.

The time was transformed from (ms) to (s) by dividing t by 1000.

T=0 was set as the moment of application of the compound.

To calculate the **frequency**, the interval between following events was determined (delta t). By dividing 1 by delta t, an individual frequency was determined. This is completely different from dividing the total number of events by the interval in which they occurred. In the method that is been used here, the weight of every event is the same.

It should however be realized that this may lead to some problems. Sometimes, a single "real" event might have been interpreted as two single events by the programming. This leads to an immense high frequency, strongly biasing the average. Therefore, a cut-off value for frequency of 20 Hz was used, after plotting single events' frequency against time to check this. Figure 4.1 shows individual frequencies after cut-off.
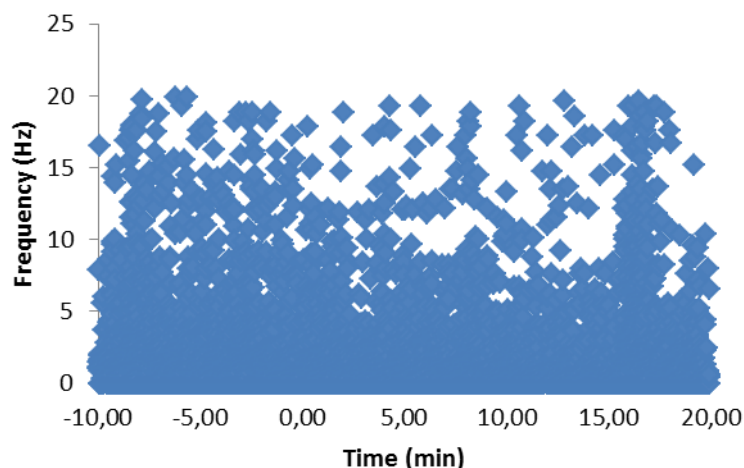

Figure 4.1: Frequency of single events after cut-off 20 Hz. *This graph shows individual frequencies after a cut-off value of 20 Hz to exclude artificial events. T0 - T10 min = NESS (0.5 uM), TTX, DNQX. T0 – T20 min = SR (1 uM), NESS (0.5 uM), TTX, DNQX. (Experiment 101020B)*

Then, averages for epochs of 2 minutes were calculated, including standard errors (by dividing the standard deviation by the square root of the number of events). An example is shown in figure 4.2. Graphs of individual events were made, in which t=0 represents addition of the compound. Graphs start at t=-10 min to show baseline activity. Averages for epochs of 2 minutes were also calculated for amplitude, including standard errors and shown in figure 4.3.
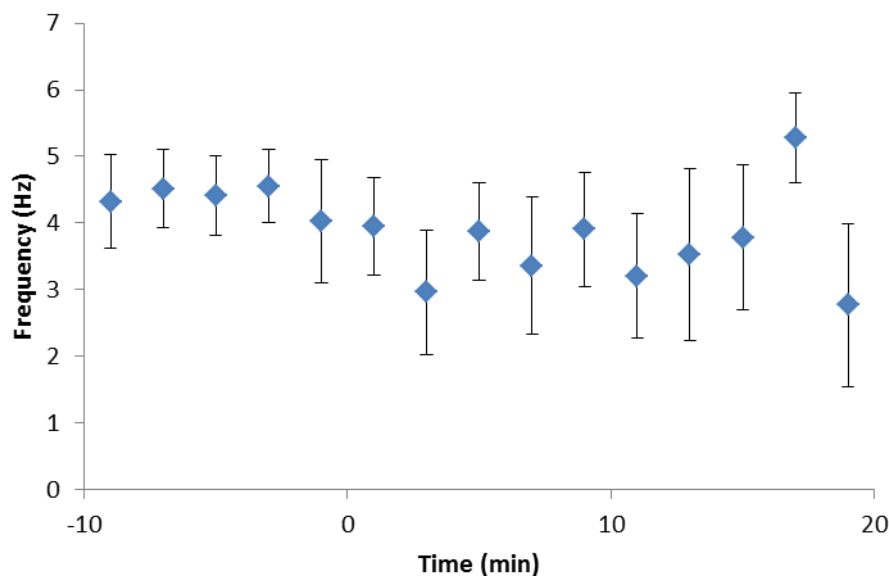

Figure 4.2: Frequency averages for 2 minute epochs of a single recording. *Frequencies of events were calculated individually before averaging in two-minute intervals. T0 - T10 min = NESS (0.5 uM), TTX, DNQX. T0 – T20 min = SR (1 uM), NESS (0.5 uM), TTX, DNQX. Standard errors were calculated by dividing the standard deviation by the square root of the number of events (Experiment 101020B)*
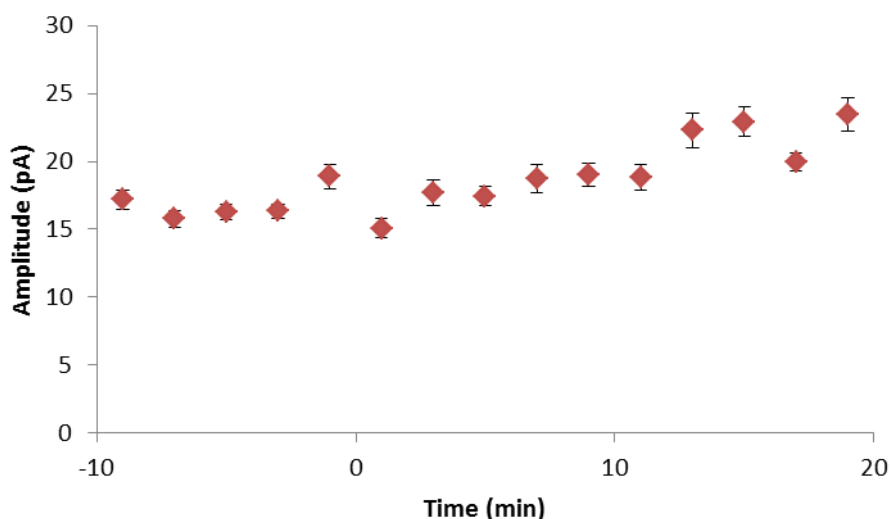
Figure 4.3: Amplitude averages for 2 minute epochs of a single recording. *Amplitudes of events were calculated individually before averaging in two-minute intervals. T0 - T10 min = NESS (0.5 uM), TTX, DNQX. T0 – T20 min = SR (1 uM), NESS (0.5 uM), TTX, DNQX. Standard errors were calculated by dividing the standard deviation by the square root of the number of events. (Experiment 101020B)*

Step 5: Processing data: multiple experiments

Differences between individual experiments did not shown convincing differences between the three treatments which are shown in the table below. The distribution of the compounds is shown.

Experiments	Treatment time < 0	Treatment time > 0
N=6	TTX, DNQX, BSA	**SR (1 uM)** + TTX, DNQX, BSA
N=7	TTX, DNQX	**NESS (0.5 uM)**, TTX, DNQX
N=4	***NESS (0.5 uM), TTX, DNQX***	***SR (1 uM), NESS (0.5 uM), TTX, DNQX***

The next step in analyzing the data was combining multiple experiments of the same treatment. In all experiments, time of addition of compound was set to zero. Combining was done by averaging the two-minute intervals (epochs). However, to correct for differences in basal activity, the basal activity (the five epochs before t=0) of a single experiment was set to one. Thereby each epoch of this experiment was calculated relative to this basal activity (including the epochs before t=0 that together define the basal activity). The frequencies, relative to their basal activity, were averaged per epoch. The same was done for amplitude. Standard errors were calculated dividing standard deviation by the square root of the number of experiments. These results are shown in the following figures 5.4 - 5.9.
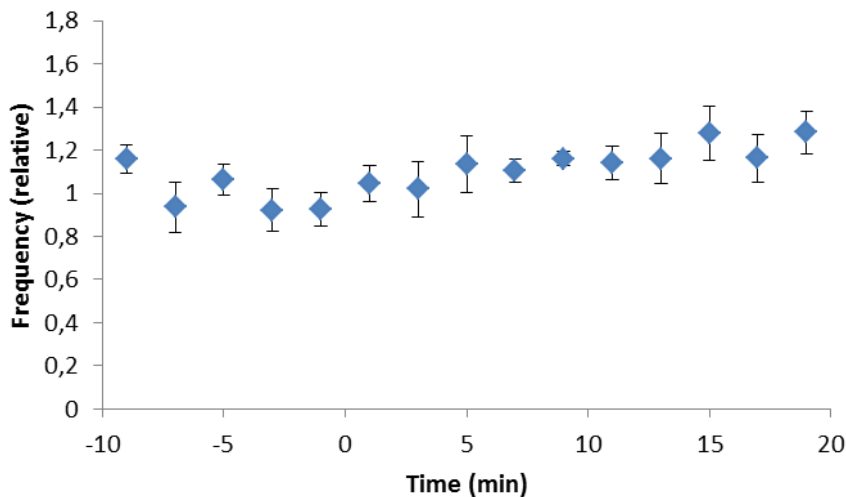

Figure 5.4: Average frequency by addition of SR141716A. *Time < 0:* TTX, DNQX. Time > 0: **SR (1 uM)** + TTX, DNQX (N=4). The effect of SR application on frequency is not very clear.
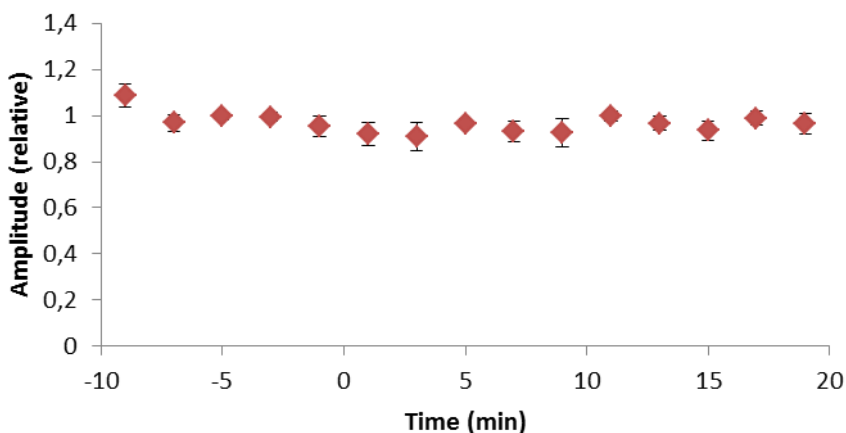

Figure 5.5: Average amplitude by addition of SR141716A. *Time < 0:* TTX, DNQX. Time > 0: **SR (1 uM)** + TTX, DNQX (N=4). Amplitude seems to be unaffected by SR.
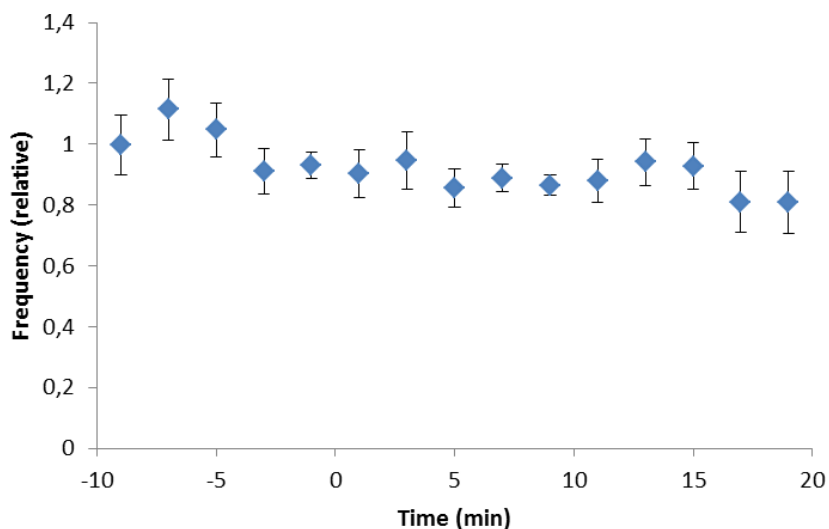
Figure 5.6: Average frequency by addition of NESS0327. *Time < 0:* TTX, DNQX. Time > 0: **NESS (0.5 uM)**, TTX, DNQX. (N=7). The effect of NESS application on frequency is not very clear.
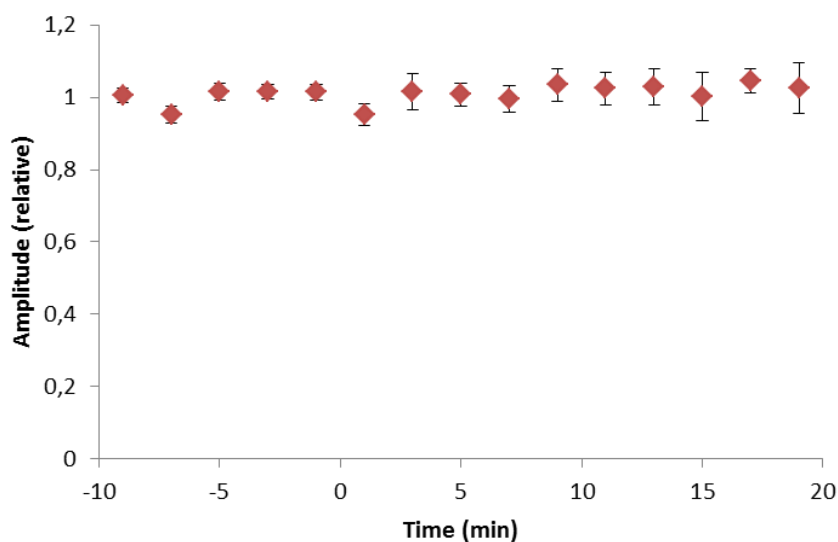

Figure 5.7: Average amplitude by addition of NESS0327. *Time < 0:* TTX, DNQX. Time > 0: **NESS (0.5 uM)**, TTX, DNQX. (N=7). Amplitude seems to be unaffected by the NESS.
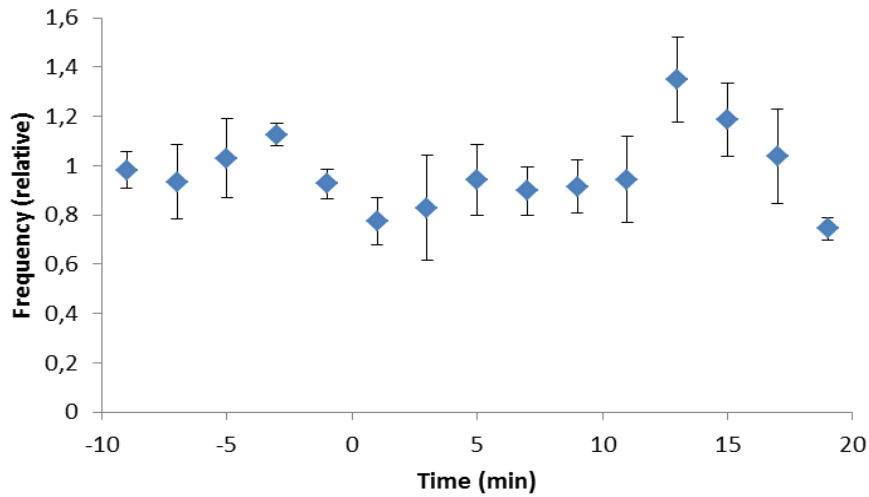
Figure 5.8: Average frequency by addition of SR on top of basal presence of NESS0327.
Time < 0: **NESS (0.5 uM), TTX,** *DNQX.* Time > 0: **SR (1 uM), NESS (0.5 uM),** *TTX, DNQX.*
(N=4). The effect of SR application over NESS on frequency is not very clear.
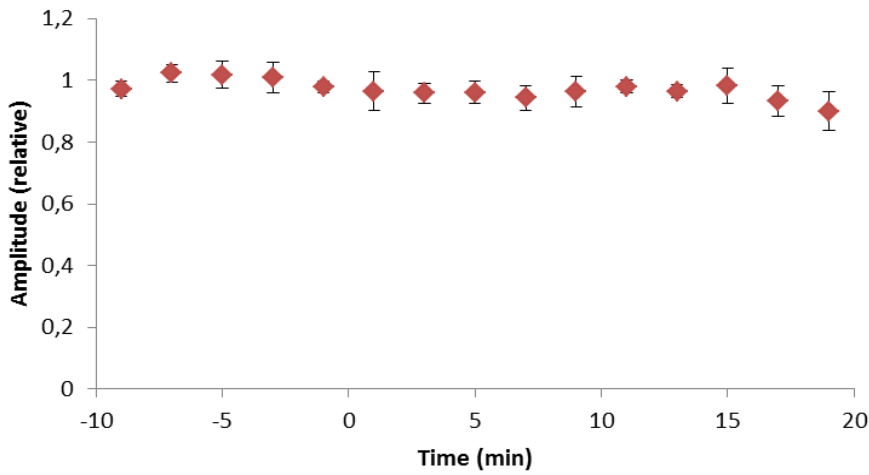

Figure 5.9: Average amplitude by addition of SR on top of basal presence of NESS0327.
Time < 0: **NESS (0.5 uM),** *TTX, DNQX.* Time > 0: **SR (1 uM), NESS (0.5 uM),** *TTX, DNQX.*
(N=4). Amplitude seems to be unaffected by the addition of SR to NESS.

Results and Conclusion

Effects on EPSC Frequency

Averaged frequency effects, as shown in figure 5.4, 5.6 and 5.8 are not very outspoken. Therefore, the results were reduced even more. Figure 6.1 shows a bar graph, in which average basal activity (t=-10 to t=0) is compared to the interval after treatment (t=10 to t=20). SR seems to increase frequency with a factor 1,2. NESS shows a decrease and the addition of SR in earlier presence of NESS seems to have little effect.

It should be mentioned that the calculated averages, including those in the earlier chapters were not calculated Log transformed. Furthermore, statistical information was lost per step of averaging (both averaging the average of an epoch in an individual experiment and averaging those averages themselves). Furthermore, the choice what to compare with baseline activity [t=-10 to t=0], in this case [t=10 to t=20], might be crucial for the results, since the effect might differ over time.
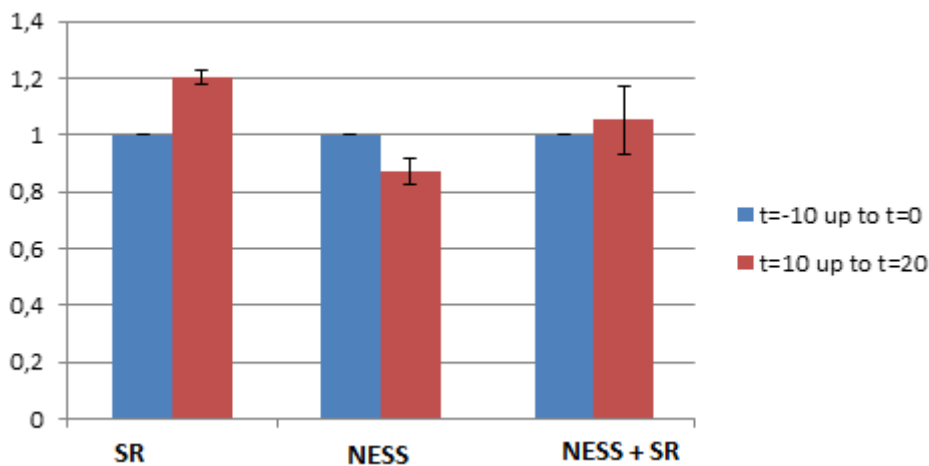

Figure 6.1: Frequency: averaged relatives before and after SR and/or NESS application. *Average frequency of the period t=-10 to t=0 was set 1 for individual experiments. The amplitude average after application of either SR(N=6), NESS(N=7) of both(N=4) [t=10 to t=20] was calculated relative to [t=-10 to t=0]. Since these relatives were calculated before averaging them, standard errors from t=-10 to t=0 are lacking, since they were all 1. Frequency seems to be affected by SR. NESS seems to have no effect. SR in addition to NESS is the only treatment in which the averaga frequency seems to be decreased.*
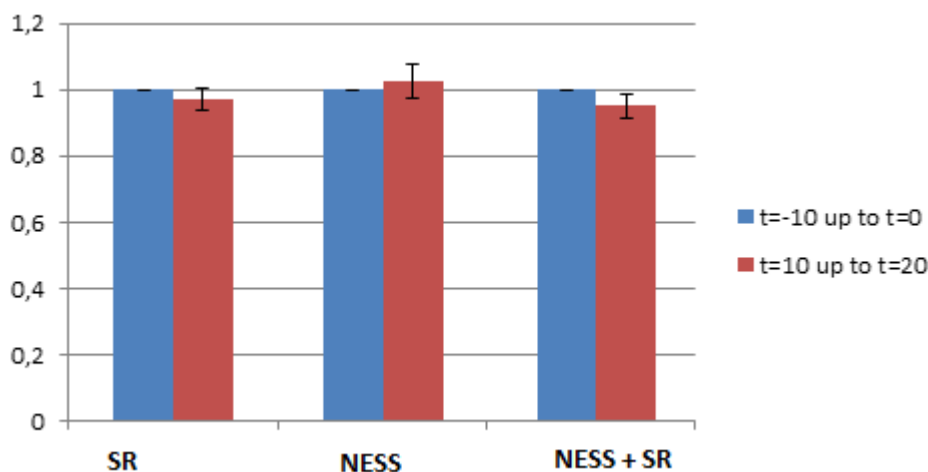

Figure 6.2: Amplitude: averaged relatives, before and after SR and/or NESS application. *Average amplitude of the period t=-10 to t=0 was set 1 for individual experiments. The relative amplitude average after application of either SR(N=6), NESS(N=7) of both(N=4) [t=10 to t=20] was calculated relative [t=-10 to t=0]. Since these relatives were calculated before averaging them, standard errors from t=-10 to t=0 are lacking, since they were all 1. Amplitude seem not to be affected by either SR, NESS, or SR in addition to NESS.*

46

Effects on EPSC amplitude

As might already have been concluded from figures 5.5, 5.7 and 5.9, there seems to be no amplitude effect in either of the treatments. In figure 6.2, the same protocol was used as in figure 6.1. These seems to be hardly an effect between the [t=-10 to t=0] and [t=10 to t=20] interval.

Conclusion

The practical set-up of an experiment was shown in the steps 1, 2 and 3. Results found by a comparable experimental set-up were used and processed in steps 4 and 5.

It was hypothesized that SR141716A (SR) would have a stronger effect on EPSC frequency in the VTA, compared to NESS0327 (NESS). Because endocannabinoids act presynaptic, effects on amplitude were not expected. Indeed, absence of effects on amplitude was found. In contrast, results on frequency are not very clear and incompatible with theory. It could be argued that tweaking statistical parameters over and over again, to match theory, is just unfair. In this case however, fine-tuning the statistical calculations, which has been mentioned, might lead to more realistic results.